Multiplex-edited mice recapitulate woolly mammoth hair phenotypes

Rui Chen[1], Kanokwan Srirattana[1], Melissa Coquelin[1], Rafael Vilar Sampaio[1], Raphael Wilson[1], Rakesh Ganji[1], Jacob Weston[1], Alba Ledesma[1], Jessie Beebe[1], Jacob Sullivan[1], Yiren Qin[1], Chris Chao[1], Jamie Papizan[1], Anthony Mastracci IV[1], Ketaki Bhide[2], Jeremy Mathews[2], Rorie Oglesby[1], Mitra Menon[2], Tom van der Valk[3, 4], Austin Bow[1], Brandi Cantarel[2], Matt James[1], James Kehler[1,5], Love Dalén[3, 4, 6], Ben Lamm[1,2], George Church[1, 2, 7], Beth Shapiro[1*], Michael Abrams[1*]

[1] Colossal Biosciences, Dallas TX, USA

[2] Form Bio, Dallas TX, USA

[3] Department of Bioinformatics and Genetics, Swedish Museum of Natural History, Stockholm, Sweden

[4] Centre for Palaeogenetics, Svanter Arrhenius väg 20C, Stockholm, Sweden

[5] UT Southwestern Medical Center, Dallas TX, USA

[6] Department of Zoology, Stockholm University, Stockholm, Sweden

[7] Department of Genetics, Harvard Medical School, Boston, MA, USA

[*] Corresponding authors: mabrams@colossal.com; beth@colossal.com

Abstract:

The woolly mammoth (*Mammuthus primigenius*) possessed a thick woolly coat and other cold-adaptive traits that enabled survival in harsh Arctic environments. Current de-extinction efforts focus on genetically modifying the closely related Asian elephant to express woolly mammoth traits. In this study, we establish a multiplex-edited mouse model with modifications in genes associated with hair morphology and lipid metabolism, enabling insights into traits involved in developing woolly hair and cold tolerance. Our optimized workflows achieved high editing efficiencies and produced genetically modified mice with simultaneous editing of up to seven different genes. Selected modifications include loss-of-function mutations in *Fgf5*, *Tgm3*, and *Fam83g*, among others. The resulting mice display exaggerated hair phenotypes including curly, textured coats, and golden-brown hair. This study establishes a rapid platform for testing mammoth-centric genetic variants while advancing methods for complex genetic model generation. These approaches inform de-extinction efforts and research into the genetic basis of mammalian hair development and cold adaptation.

Introduction

One of the most prominent ongoing de-extinction efforts focuses on the woolly mammoth, *Mammuthus primigenius*, which disappeared following the extinction of the last surviving population on Wrangel Island approximately 4,000 years ago [1,2]. The mammoth de-extinction project aims to resurrect key mammoth phenotypes like woolly coats and other adaptations to cold habitats by expressing mammoth-specific gene variants in cells of the closely related Asian elephant, *Elephas maximus*, followed by somatic cell nuclear transfer and surrogacy [3]. The selection of genetic variants underlying these traits proceeds through comparative genomic analysis [4] and, where possible, experimental validation of their predicted phenotypic effects. However, for mammoth de-extinction, such validation faces significant challenges. The 22-month gestation period of elephants and their extended reproductive timeline make rapid experimental assessment impractical. Further, ethical considerations regarding the experimental manipulation of elephants, an endangered species with complex social structures and high cognitive capabilities, necessitate alternative approaches for functional testing.

Mouse model systems offer a compelling alternative approach to exploring the phenotypic impact of genetic modifications proposed for mammoth de-extinction. Mice have a 20-day gestation period and well-established genetic manipulation protocols, which together enable rapid functional testing of candidate gene variants [5–7]. By introducing genetic changes identified as potentially linked to key mammoth traits, researchers can evaluate the impact of these modifications on, for example, hair growth patterns, fat distribution, and cold tolerance within a tractable experimental timeframe. While mice cannot fully replicate elephant physiology, mouse models provide valuable insight into the functional consequences of mammoth-specific adaptations and will help prioritize genetic modifications likely to confer desired traits in proboscideans.

The CRISPR/Cas9 system has revolutionized the development of genetically modified animal models [8,9]. Over the last decade, this system has evolved from simple DNA cutting tools into an increasingly versatile toolkit for precise genetic modifications [10–13]. Multiple approaches now enable efficient generation of gene-edited mice, including injection of modified murine embryonic stem cells (mESCs) into blastocysts, high-efficiency chimera production through injection of gene-edited mESCs into 8-cell stage embryos, and direct zygotic modification through electroporation [6,7,14–16]. These technical advances have accelerated the production of complex genetic models, enabling detailed *in vivo* study of gene function and has significant implications for ambitious conservation efforts such as de-extinction.

Previous studies of spontaneous and engineered mouse mutations have revealed key genetic regulators of hair development, texture, length, density, and color. These include the *Tgm3* gene that leads to wavy pelage and curly vibrissae [17], the *Fzd6* Wnt receptor that controls hair follicle orientation [18], and *Astn2*, for which the deletion of exon 5 combined with *Fzd6* loss generates a dorsal transverse hair pattern [19]. Additional genes implicated in hair phenotypes include *Fam83g*, which influences coat texture and underlies the so-called "wooly" mutation that presents as an altered rough coat texture [20], Fibroblast Growth Factor 5, *Fgf5*, which regulates hair length through control of the anagen-catagen transition resulting in growth of longer guard hair [21], and *Tgfa*, a transforming growth factor that plays a critical role in regulating hair development and for which loss of function results in wavy hair textures [22]. Mutations in keratin genes such as *Krt25* and *Krt27* also alter hair structure [23,24], and melanocortin-1 receptor (*Mc1r*) regulates pheomelanin and eumelanin production and, as a consequence, coat color [25].

Here, we generated a panel of multiplex-edited mouse models with loss of function (LOF) mutations in *Tgm3*, *Fzd6*, *Astn2, Fam83g*, *Fgf5*, *Tgfa* and *Mc1r* (**Fig. 1A**). While the majority of these genes were selected based on previous observations of coat phenotypes in mice, comparative analyses of mammoth and elephant genomes revealed a similar loss of function variant in *Tgfa* that occurred in mammoth lineage after divergence from Asian elephants. We also introduced precision missense mutations in *Krt25* and *Krt27,* the latter for which we inserted a residue that was also genetically fixed in mammoths [26]. In addition to genes associated with coat phenotype, we selected *Fabp2*, a gene involved in fatty acid trafficking that has an early stop codon in mammoths [27]. In mice, disruption (knock-out or KO) of *Fabp2* leads to sex-dependendent metabolic perturbations and differences in adiposity [28,29], suggesting a role in cold adaptation. We employed direct zygote editing (Experiments A, B, and C) and high-efficiency chimera approaches (Experiments D and E) to produce mice bearing as many as eight homozygous edits in seven different genes (**Fig. 1B, Table 1**). These novel combinations of genetic modifications yielded mice with a number of hair phenotypes, including woolly coat textures, providing valuable models for both mammoth de-extinction efforts and basic studies of hair follicle biology.

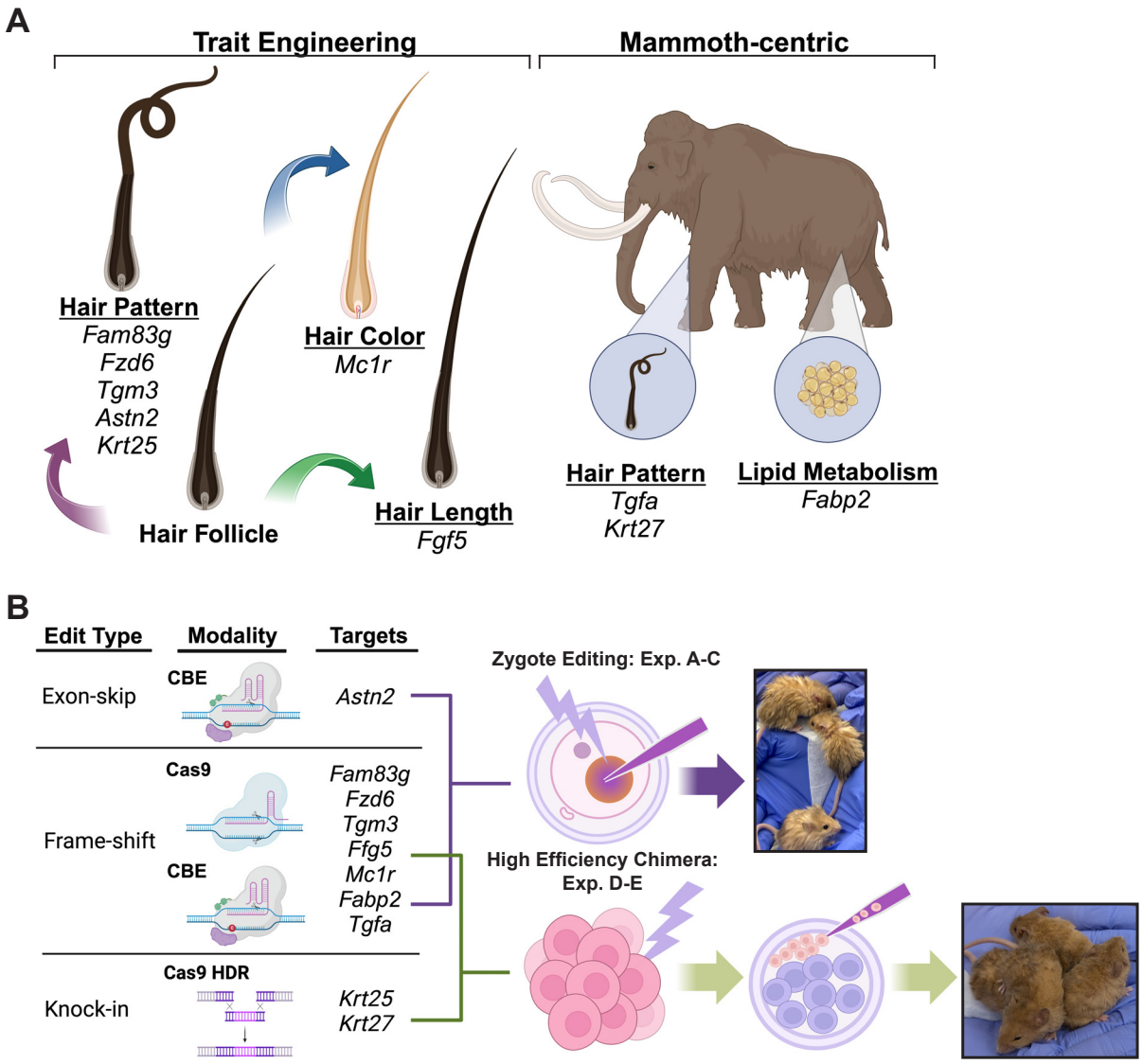

Fig. 1. Overview of target traits, target genes and editing workflows. Also see Table 1. **(A)** The target genes in this study fall into two categories: woolly hair trait engineering based on existing literature and mammoth-centric edits. **(B)** An illustration summarizing the editing modalities and two correlated animal generation workflows.

Table 1. Major trait engineering target genes in this study

Gene	Expected Phenotype	Edit type	Modality used	Workflow		Experiment
Astn2	Ridge hair	Exon-skip KO	CBE	Zygote editing		C
Fam83g	Woolly hair	Frame-shift KO	Cas9; CBE	Zygote editing		A B C
Fzd6	Disoriented hair	Frame-shift KO	Cas9; CBE	Zygote editing		A C
Tgm3	Curly hair	Frame-shift KO	Cas9; CBE	Zygote editing		B C
Fgf5	Long hair	Frame-shift KO	Cas9; CBE	Zygote editing	High efficiency chimera	A B C D E
Mc1r	Gold hair	Frame-shift KO	Cas9; CBE	Zygote editing	High efficiency chimera	A B C D E
Fabp2	Lipid metabolism; Mammoth-centric	Frame-shift KO	Cas9; CBE	Zygote editing	High efficiency chimera	A B C D E
Tgfa	Wavy hair; Mammoth-centric	Frame-shift KO	Cas9		High efficiency chimera	D E
Krt25	Curly hair	KI	Cas9 HDR		High efficiency chimera	D E
Krt27	Textured hair; Mammoth-centric	KI	Cas9 HDR		High efficiency chimera	D E

Results and Discussion

Experiments A and B: Direct Multiplex Editing of Zygotes with CRISPR/Cas9

Electroporation of CRISPR/Cas9 ribonucleoprotein (RNP) into mouse single-cell zygotes achieved efficient disruption of the six targeted genes: *Fgf5*, *Mc1r*, *Fam83g*, *Fzd6*, *Tgm3, and Fabp2* (**Figs. 1B, 2A, 2B**). We carried out screening assays to prioritize sgRNAs based on three criteria: 1) high editing efficiency, 2) low predicted risk of off-target edits, and 3) targeting positions that either closely mimic previously reported mutations or that are in an early exon so as to facilitate full knock-out (KO).

To assess editing efficiency for multiple sgRNAs per target gene, we electroporated thawed B6C3F1 × B6D2F1 zygotes with Cas9 ribonucleoprotein complexes. We then cultured embryos to the blastocyst stage, followed by collection for genomic analysis (**Fig. 2A**). **Fig. 2B** shows the editing efficiencies (% total modifications and KO) of each sgRNA, which ranged from undetectable to 100% editing and highlights sgRNAs selected for subsequent assays in orange. Binding sites of the selected sgRNA within each target gene are shown in **Fig. S1A**.

We carried out two Cas9 editing animal production experiments using the selected sgRNAs (**Table 2**). In Experiment A, we electroporated freshly collected B6SJLF2 zygotes with Cas9 RNPs and sgRNAs targeting *Fgf5*, *Mc1r*, *Fzd6, Fam83g*, *Fabp2*. Nearly half of zygotes (63/134) developed to the blastocyst stage following electroporation (**Table 2**). We then transferred 60 blastocysts to three ICR pseudo-pregnant surrogates (**Fig. 2A**). Eleven pups were born (18%; **Table 2**). Genotyping confirmed successful KO across all five target genes (**Fig. 2C**), with an average editing efficiency per gene across the 11 pups ranging from 80% for *Mc1r* to 94% for *Fam83g* (**Fig. 2C**). Only modest mosaicism was detected: 44/55 of the possible target sites (5 targets x 11 mice) were edited at a frequency of more than 80%. The detailed genotypes of two mice are shown in **Fig. 2D**. Specifically, all five target genes were fully disrupted (homozygous KO) in mouse #512, while mouse #517 had a homozygous in-frame 9-bp deletion in *Fzd6* but homozygous KO for the other four target genes.

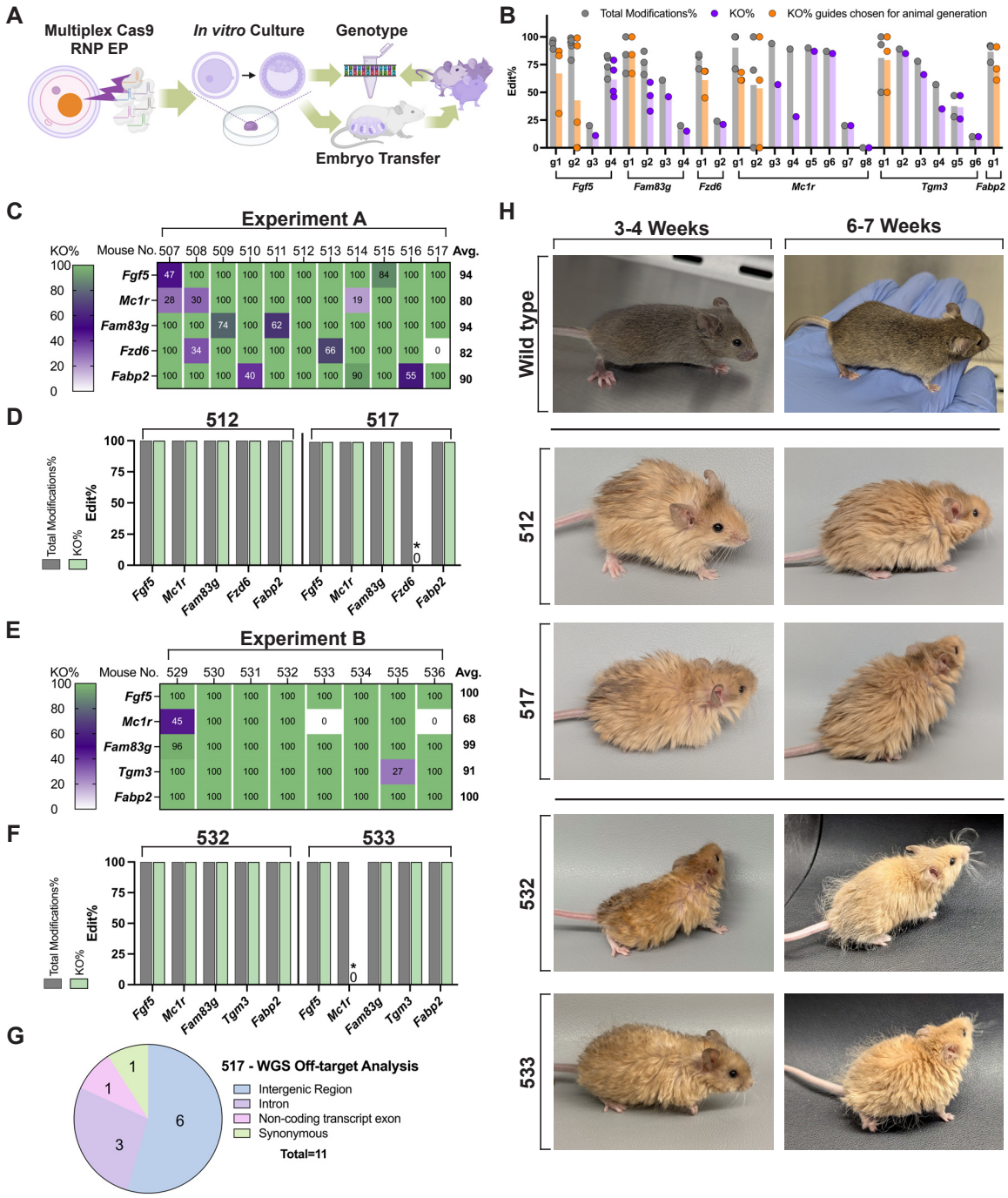

Fig. 2. Experiments A and B: Gene editing in mice using CRISPR/Cas9 RNP zygote electroporation. (A) Workflow. We electroporated (EP) a pool of Cas9 RNPs with synthetic sgRNAs into wild-type mouse zygotes. We then cultured embryos into blastocyst stage *in vitro* and genotyped all blastocysts to estimate editing efficiencies. Next, we transferred blastocysts into surrogates for animal production experiments. Finally, we collected and genotyped ear punches from pups 21 days after birth. **(B)** Guide screening. We designed between one and eight guides for each target gene and screened each guide for editing efficiency in terminal experiments. For each guide, mean total modification efficiency (KO + unintended edits) is presented as a gray bar, KO efficiency as a purple bar for guides not selected for animal production experiments, and orange bar for guides selected for animal production experiments. Bars present average efficiencies from at least five embryos. Each circle represents an individual experiment that includes data from single embryos to pools of up to 18 embryos. **(C, E)** The KO% profiles of mice

generated from Experiments A and B. Each column represents one mouse. “Mouse No.” is the name of the mouse used in this study. **(D, F)** The total modifications% and KO% from mice #512 and #517 of Experiment A and #532 and #533 of Experiment B. “*” highlights the two in-frame homozygous edits in #517 (a 9 bp deletion in *Fzd6*) and #533 (a 21 bp deletion in *Mc1r*). **(G)** Editing off-target analysis by whole genome sequencing on mouse #517. **(H)** Photos of mice #512 and #517 of Experiment A and #532 and #533 of Experiment B at 3-4 weeks old and 6-7 weeks old. The wild-type reference photos are from age-matched agouti B6SJL F2.

In Experiment B, we efficiently produced mice with simultaneous disruption (KO) of *Fgf5*, *Mc1r*, *Fam83g*, *Tgm3,* and *Fabp2* (**Fig. 2E**). We electroporated zygotes as in Experiment A, resulting in a blastocyst formation rate of 56% (42/75; **Table 2**). Of these blastocysts, 28 were transferred to two ICR surrogates, and eight pups were born, yielding a 29% birth rate (8/28; **Table 2**). Comparable levels of editing were achieved for the four gene targets in common with Experiment A. We detected little mosaicism, as only 4/40 possible sites (8 mice x 5 targets) were edited at less than 95%. The unique target gene for this experiment, *Tgm3*, was edited at 100% in seven out of eight mice. The average editing efficiency per gene was 92%, and the average editing efficiency per animal was 93%. The detailed genotypes of two mice, #532 and #533, are shown in **Fig. 2F**.

Table 2. Summary of the gene targets, number of zygotes, and edited mice obtained after Cas9 electroporation

Experiment	Gene Targets	Blastocyst rate (%)	No. of recipients	No. pups born/ No. transferred (%)	No. live pups/ No. pups born (%)
A	*Fgf5*, *Fabp2*, *Mc1r*, *Fzd6*, *Fam83g*	63/134 (47)	2	11/60 (18)	11/11 (100)
B	*Fgf5*, *Fabp2*, *Mc1r*, *Fam83g*, *Tgm3*	42/75 (56)	2	8/28 (28)	8/8 (100)

We performed short-read whole genome sequencing of mouse #517 to investigate the frequency of off-target edits. For the selected guides, computational analysis predicted 282 sites with three or fewer guide mismatches against the mouse genome where off-target edits were most likely to occur. We identified only 11 off-target edits in mouse #517 at these sites, none of which resulted in missense mutations (**Fig. 2G)**.

Experiments A and B produced mice with a variety of coat and eye colors determined by the status of *Mc1r* editing and whether the *Oca2*^{p} and *Tyr*^{c} loci, which are heterozygous in B6SJL F1 mice, are homozygous or heterozygous (**Fig. 2H**, **Figs. S1C and S1D**, **Figs S2-5**). Coat colors of unedited B6SJL F2 include agouti, black, light gray, white, and cream depending on which alleles for *Asip*, *Oca2*, and *Tyr* are inherited (**Fig. S1B**) [30,31]. *Oca2*$^{p/p}$ mice have red eyes and light gray or cream coats, depending on which agouti (*Asip*) allele is present [32,33],

while *Tyr*$^{c/c}$ mice have red eyes and white coats [34]. Unedited mice with agouti or black coats have black eyes [35]. As such, our intended disruption of *Mc1r* should only alter black or agouti coats to gold coats [25,36].

We successfully knocked out *Mc1r,* resulting in gold mice with black eyes. This phenotype is observed in mice #511, #512, #513, #516, #517, #531, #532, #533, #534, and #535. Mice #509, #510, #515, and #530 were also homozygous knockouts at *Mc1r* but had white coats (**Figs. S1C and S1D**), as expected in mice variants for albino coats [37]. Two mice with disrupted *Mc1r* do not show the expected coat color phenotype. Mouse #533 had a 21 bp in-frame deletion in *Mc1r* but a gold coat (**Fig. 2H**, **Fig. S5**), indicating that the disruption still knocked out the gene. Mouse #536 also had a 21 bp in-frame deletion of *Mc1r* but presented with black hair (**Fig. S1D**). The *Mc1r* deletion in mouse #536 was, however, shifted by +9 bp compared to that of mouse #533. When we aligned both to the wild-type MC1R protein (**Fig. S1E**), we observed that the deletion in mouse #536 occurred near the second transmembrane domain of MC1R and spans the E92 residue, the loss of which had been associated previously with black coat color [38].

Both Experiments A and B produced mice with long hair, enhanced waviness, and altered coat texture compared to wild type (**Fig. 2H**, **Figs. S1C and S1D**, **Figs S2-5**). These phenotypes are as expected from the target edits. Long hair is the predicted outcome of disruption to *Fgf5* in exon 1 [21], for example, and disruptions to *Fam83g, Fzd6*, and *Tgm3* were all associated previously with changes to hair texture [17,18,20]. In *Fam83g,* for example, the previously described “wooly” (*wly*) phenotype is thought to be caused by altered splicing that leads to a frameshift mutation in exon 4 [20] and a shortened protein. Our *Fam83g* sgRNA produces a similar change by targeting a disruption to the first few nucleotides of exon 3. We observed a feathered hair texture in our *Fam83g*-edited mice, supporting the hypothesis that the truncation of this protein alters hair development. In *Tgm3,* the wellhaarig variant we4j is a 7 bp deletion that leads to a truncation after residue 512 [17]. Our *Tgm3* sgRNA targets within 40 bp downstream of we4j, leading to a similar frameshift. Experiment B mice with homozygous editing of *Tgm3* had curlier coats than Experiment A mice, which were not edited at *Tgm3*. Deletion of *Fzd6* has been shown to alter hair follicle patterning [18], and all our mice with *Fzd6* knocked out show the predicted phenotype. However, mice #517 (**Fig. 2H**, **Fig. S3**) and #513 (**Fig. S1C**) had incomplete disruption of *Fzd6,* either as an in-frame mutation (#517) or mosaicism (#513), yet still had a woolly/wavy coat, suggesting impact from other simultaneous edits. Future experiments will be necessary to explore the contribution of each edit to the coat phenotype.

Experiment C: Direct Multiplex Editing of Zygotes with cytosine base editors

In Experiment C, we used cytosine base editors (CBE) to knock out seven genes simultaneously: *Fgf5*, *Mc1r*, *Fam83g*, *Fzd6*, *Tgm3*, *Astn2*, and *Fabp2* (**Fig. 1B**, **3A and 3B**). CBE deaminates cytosine (C) to thymidine (T) within a defined targeting region [39]. CBE can precisely install premature stop codons (*Fgf5*, *Mc1r*, *Fam83g*, *Fzd6*, *Tgm3*, and *Fabp2*) [40] or mutate splice sites for creating gene truncations and deletions (*Astn2*) [19,41] without eliciting double-stranded breaks [39].

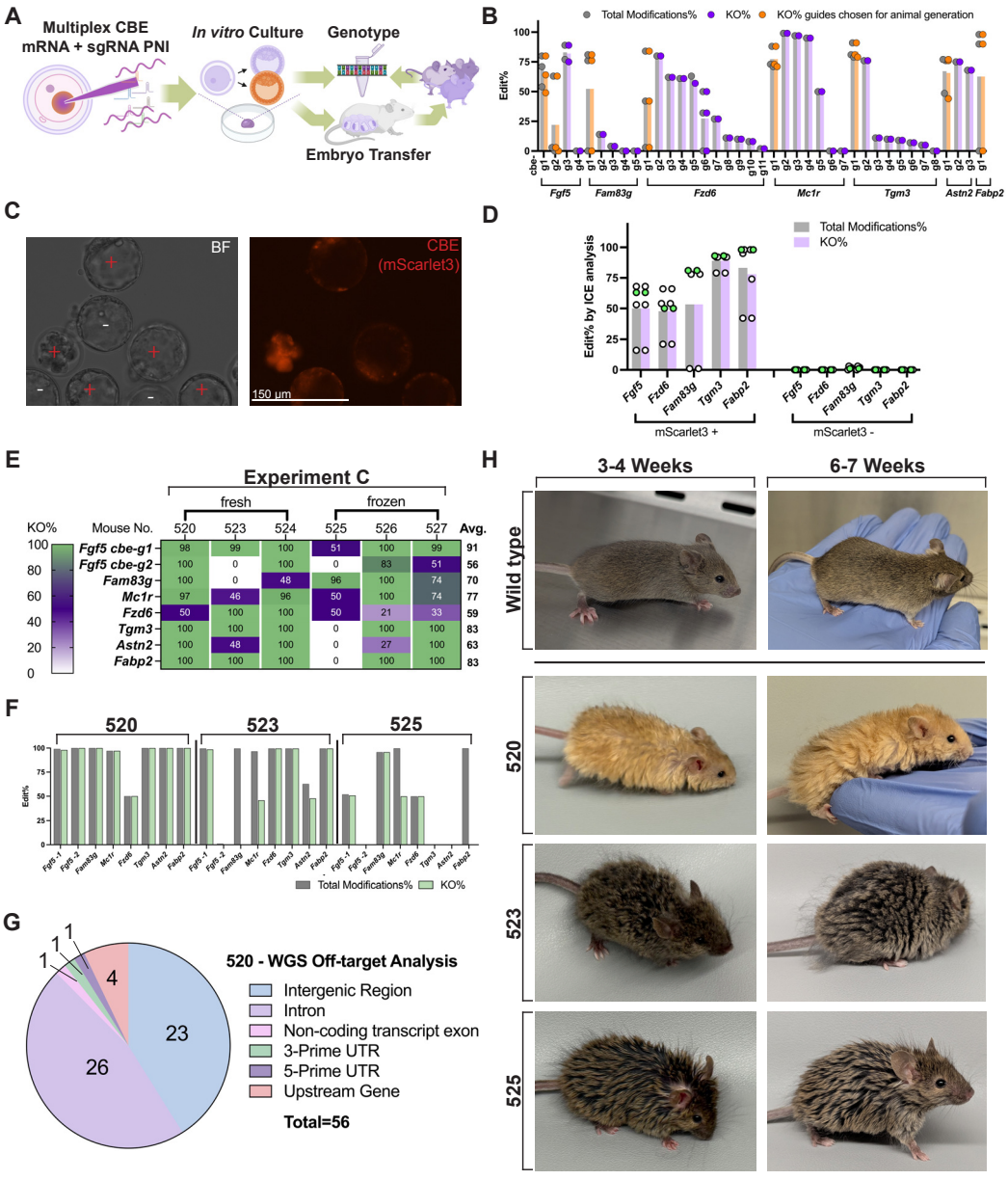

Fig. 3. Experiment C: multiplex editing in mice using Cytosine Base Editor (CBE) PNI. (A) Workflow. We delivered a pool of CBE mRNA with sgRNAs into wild-type mouse zygotes by pronuclear injection (PNI). The mRNA

transcript co-expresses CBE and a red fluorescent protein, mScarlet3. We cultured the embryos to the blastocyst stage *in vitro* and then evaluated mScarlet3 fluorescence. For screening experiments, we genotyped all blastocysts. For animal-producing experiments, we selected healthy blastocysts with bright mScarlet3 signals for transfer into surrogates. We collected ear punches for genotyping 21 days after the birth of the pups. **(B)** Guide screening. We designed between one and eleven guides for each of the target genes and screened each guide for editing efficiency in terminal experiments. For each guide, mean total modification efficiency (KO + unintended edits) is presented as a gray bar, KO efficiency as a purple bar for guides not selected for animal production experiments, and an orange bar for guides selected for animal production experiments. Bars present average efficiencies measured from at least six embryos. Each circle represents an individual experiment, including data from single embryos to pools of up to 19 embryos. **(C)** Fluorescent images of blastocysts after PNI of CBE-P2A-mScarlet3 mRNA and sgRNAs. Left: red signal from mScarlet3; right: bright field (BF) showing all embryos. "+" highlights the red embryos, and "-" highlights the non-red embryos. **(D)** Mean total modifications% (grey bars) and KO% (purple bars) comparison between mScarlet3+ and mScarlet3- embryos. Bars include data from at least seven embryos. White circles represent data from single embryos; green circles represent data from 6-8 pooled embryos. **(E)** The KO% profiles of mice generated from the CBE animal production Experiment C. Each column represents one mouse. "Mouse No." is the designated name of the mouse used in this study. **(F)** The total modification% and KO% from mouse #520, #523, and #525 from Experiment C. **(G)** Off-target analysis by whole genome sequencing on mouse #520. **(H)** Photos of mouse #520, #523, and #525, from Experiment C, taken at 3-4 weeks old and 6-7 weeks old. The wild-type reference photos are from age-matched agouti B6SJL F2; the same images as in Fig. 2(H).

To evaluate the efficiency of our CBE sgRNAs, we microinjected thawed F2 hybrid zygotes with *in vitro* transcribed CBE mRNA and chemically synthesized sgRNA, and collected embryos at blastocyst stage for genomic analysis (**Fig. 3A**). We found that cytosine deamination varied depending on the sgRNA and the target gene (**Fig. 3B**). We prioritized sgRNAs for animal production experiments (**Fig. 3B** orange bars, **Fig. S6A**) using the selection criteria described above.

We found that the co-expression of a red fluorescent protein, mScarlet3 via a P2A linkage was an effective reporter for CBE editing activity in zygotes (**Figs. 3C and 3D**, **Figs. S6B and S6C**). We microinjected thawed F2 hybrid zygotes with CBE editor and multiplexed sgRNAs targeting *Fgf5*, *Fzd6*, *Fam83g*, *Tgm3*, and *Fabp2*. We manually sorted blastocysts into two groups based on the presence (+) or absence (-) of the red fluorescence signal. Genotyping analysis confirmed successful base editing in all red fluorescence (+) embryos as well as high multiplexing in single embryos (**Fig. 3D** white dots, **Figs. S6B and S6C**). In contrast, embryos lacking red fluorescence (-) showed no detectable gene editing.

We leveraged the CBE reporter system to create mice edited in *Fgf5, Mc1r, Fam83g, Fzd6, Tgm3, Astn2*, and *Fabp2*. Fresh and thawed embryos exhibited comparable blastocyst formation rates: 70% (78/111) in fresh embryos and 71% (46/65) in thawed embryos (**Table 3**). Of these, the fluorescence rate of embryos was 65% (51/78) in fresh embryos and 44% (16/36) in thawed embryos. Five pups were obtained from the fresh zygote group after transferring 47 fluorophore-positive embryos (11%; 5/47), and three pups were born from the thawed group (33%; 3/9; **Table 3**). Every pup had at least heterozygous editing at more than one locus, and multiple pups were homozygous at 5-6 loci, with an average KO rate of 73% across six mice

(**Fig. 3E**). Average KO efficiencies per gene across all mice ranged from 59% for *Fzd6* to 91% for *Fgf5*. Mice #520 and #524 were edited for all seven genes. Mice #520 and #524 had homozygous KO for six genes and were heterozygous at a seventh, *Fzd6* and *Fam83g,* respectively (**Fig. 3E, Fig. S6D**). Due to our high editing efficiency and the nuclease-free nature of CBE, total gene editing (intended edits + bystander edits + indels) often matched precision stop codon installation, as few unintended insertions or deletions were detected (**Fig. 3F**, #520).

Table 3. Summary of number of zygotes, and edited mice obtained after CBE pronuclear injection

Experiment	Strain background	Zygote Status	No. blastocyst/ No. injected zygotes (%)	No. editor+/ No. blastocyst (%)	No. of recipients	No. pups born/ No. transferred (%)	No. live pups/ No. pups born (%)
C	(B6 × SJL)F1 × (B6 × SJL)F1	Fresh	78/111 (70)	51/78 (65)	3	5/47 (11)	5/5 (100)
	(B6 × C3H)F1 × (B6 × D2)F1	Thawed	46/65 (71)	16/46 (44)	1	3/9 (33)	3/3 (100)

Multiplexed CBE editing in zygotes led to few off-target edits. Our WGS analysis of 1,869 computationally predicted off-target sites revealed 56 total off-target edits in mouse #520 (**Fig. 3G**), none of which resulted in missense mutations. The higher number of predicted and observed off-target sites in Experiment C compared to Cas9 editing was as expected due to the less stringent PAM requirements of the SpRY-based editor used in Experiment C, which provides flexibility in targeting but more promiscuous editing [42].

Experiment C produced mice with similarly altered phenotypes as in Experiments A and B (**Fig. 3H**, **Fig. S6D**, **Figs. S7-9**), and both fresh (#520, #523, #524) and thawed (#525, #526, #527) embryos generated mice with comparable genotype to phenotype correlations. We observed that the addition of early stop codons in *Fgf5, Fam83g, Fzd6,* and *Tgm3* and skipping an exon in *Astn2* yielded an exaggerated hair phenotype (**Figs. 3F and 3H**, **Fig. S7**). Due to the lower editing efficiency of *Mc1r* in Experiment C compared to Experiments A and B, we obtained more agouti mice. Interestingly, while mouse #525 had only a single gene homozygously knocked out – *Fam83g* – this mouse still had a feathered coat phenotype, providing additional evidence for the role of this gene in hair development (**Fig. 3F**, **Fig. S9**). Mouse #523 was not edited at *Fam83g* (**Fig. 3F**, **Fig. S8**), and did not display a feathered coat, but rather had a frizzy/curly hair phenotype, which may be due to the additive effects of *Fgf5, Fzd6,* or *Tgm3* disruption.

Experiments D and E: Editing mESCs with CRISPR/Cas9

For Experiments D and E, we established clonal mESCs modified with genetic disruptions (KO) of *Tgfa*, *Fgf5*, and *Mc1r*, and knock-in (KI) of point mutations in the keratin family genes *Krt25* and *Krt27,* followed by chimera generation (**Fig. 4A**). *Tgfa, Krt25,* and *Krt27* were not targeted in Experiments A-C. We targeted a L86Q substitution in *Krt25* that has been associated with wavy hair in mice [23]. *Krt27* has also been linked to curly hair in mice [24] and was one of the genes highlighted by our genomic analysis, which revealed that most mammoths have a valine at amino acid position 191 while Asian elephants have a methionine. To replicate the mammoth variant at this site, we introduced a valine at the same position in mouse *Krt27*, where wild-type mice have isoleucine (**Fig. S10A**). We designed sgRNAs for Cas9 to target each gene as well as single-stranded oligonucleotide donors (ssODN) to act as HDR templates for *Krt25* and *Krt27* (**Fig. 4B**). We used optimally performing guides and ssODNs (**Fig. 4B** orange bars, **Fig. S10B**) for subsequent mESC editing experiments.

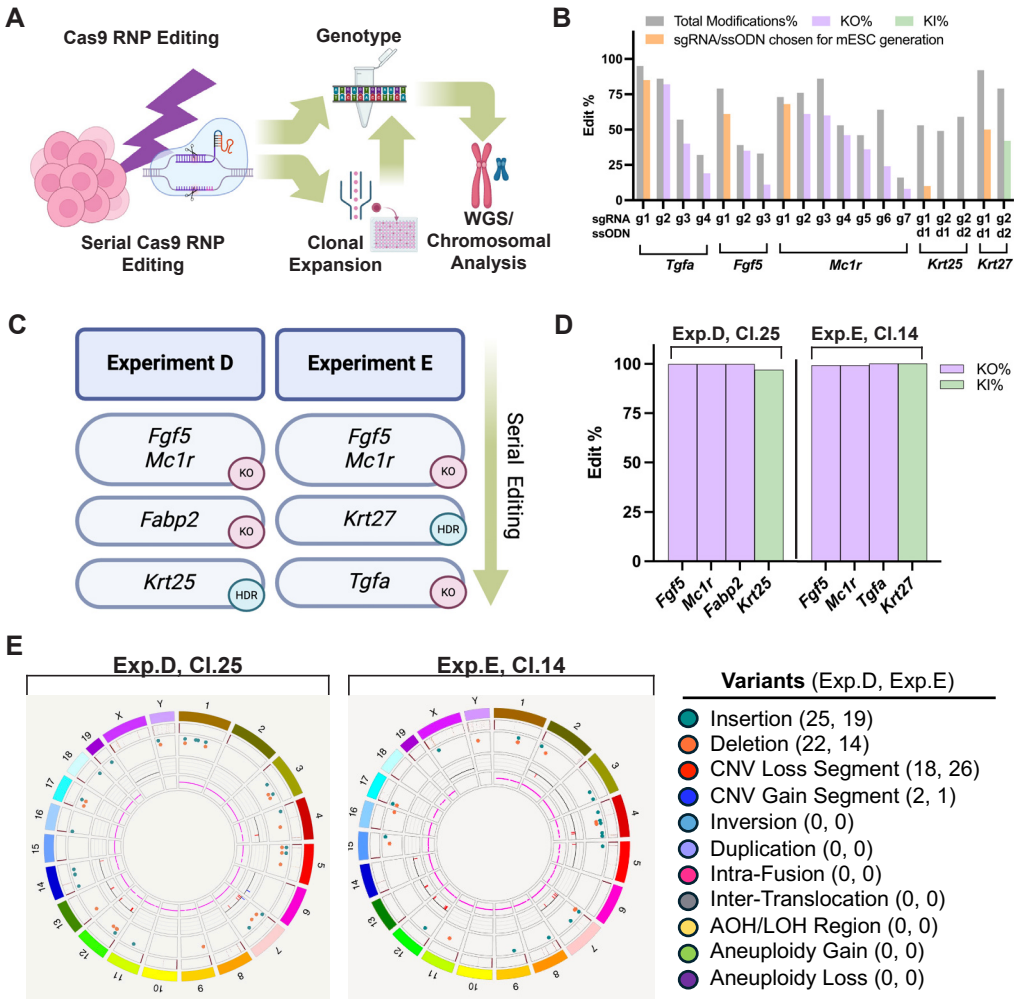

Fig. 4. Experiment D and E: generation of monoclonal, multiplex edited mouse embryonic stem cells using CRISPR/Cas9 RNP for woolly hair trait engineering. (A) Schematic for the generation of multiplex-edited monoclonal mESCs by CRISPR/Cas9 mediated KO or knock-in (KI). We electroporated mESCs with Cas9 RNPs, sgRNAs and ssODN (HDR template). We collected cells 48 hours post-transfection for genotyping by Sanger sequencing. We also single-sorted the bulk population of transfected mESCs into 96-well plates containing iMEF feeders for clonal expansion, genotyping, and karyotyping. **(B)** Guide and ssODN screening. We designed between one and seven guides for each of the target genes, and two ssODNs for genes undergoing HDR KI. For each guide, total modification efficiency is presented as a gray bar. KO (*Tgfa*, *Fgf5,* and *Mc1r*) or KI (*Krt25* and *Krt27*) efficiency is presented as a purple or green bar, respectively, for designs not selected for animal production experiments, and an orange bar for designs selected for animal production experiments. Bars of each guide or each guide-ssODN combination includes data from one experiment from two thousand mESCs. **(C)** Flowchart depicting the sequential editing strategy used to generate multiplex-edited monoclonal mESC lines. **Experiment D** was first electroporated with a pool of Cas9 RNPs targeting *Fgf5 KO* and *Mc1r KO*, followed by a single Cas9 RNP targeting *Fabp2 KO*, and a single Cas9 RNP with ssODN targeting *Krt25 KI*. **Experiment E** was first electroporated with a pool of Cas9 RNPs targeting *Fgf5 KO* and *Mc1r KO*, followed by a single Cas9 RNP with ssODN targeting *Krt27 KI*, and a single Cas9 RNP targeting *Tgfa KO.* **(D)** Bar graph showing KO% (purple) and KI% (green) for selected clonal lines generated in Experiments D and E. We collected cells from laminin-coated plates to ensure no iMEF contamination during genotyping by Sanger sequencing. Editing efficiencies were also confirmed by NGS. **(E)** Bionano Circos plot summarizing structural variations in Experiment D and E monoclonal mESC lines. Starting from the outer rings, the Circos tracks depict 1. Cytoband, 2. mm39 DLE-1 SV mask, 3. Structural variants, 4. Copy number variants, and 5. Variant allele fraction segments. Translocations would be depicted as curved lines across the center of the plot, though none were detected in either sample. Numbers of variants are summarized on the right.

We developed edited clonal mESC lines via three serial transfections targeting either *Fgf5, Mc1r, Fabp2*, and *Krt25*, or *Fgf5, Mc1r, Krt27,* and *Tgfa*, respectively (**Fig. 4C**). Post-transfection bulk cell populations included edits at all desired loci with varying efficiencies (**Fig. S10C**). Bulk cell populations were sorted to isolate single cell clones, followed by genotype screening (**Fig. 4A**). To identify fully edited clonal lines, we evaluated the editing status of 45 mESC clones for Experiment D and 48 mESC clones for Experiment E (**Fig. S10D**). To expedite the initial genotype screen, we retained mESCs on irradiated mouse embryonic fibroblasts (iMEF) feeder layers and genotyped them by Sanger sequencing. The carry-over of iMEF wild-type DNA and the detection limitation of ICE analysis for Sanger results may explain the distribution of editing (non-50% multiples) obtained. We re-genotyped promising candidates after culture on feeder-free laminin coated plates. This process identified at least one fully modified clone for each experiment – clone 25 for Experiment D and clone 14 for Experiment E (**Fig. 4D**, **Fig. S10E**).

Comparison of whole genome sequencing data from the fully edited mESCs clonal lines to wild-type mESCs revealed negligible off-target editing. As the edited clonal lines had the same genetic background (B6129), we were able to carry out an unbiased genome-wide off-target analysis by comparison to the unedited mESC line. We found no high-impact off-target variants in Experiment D, clone 25, and just one in Experiment E, clone 14 (**Table S1**), defined as splice modifying or protein coding variants. Experiment E, clone 14 had a single missense

variant in the *Prkca* gene. The annotations for all variants found in this analysis are summarized in **Table S2**.

The candidate clonal lines selected for animal generation maintained normal chromosome numbers, as assessed by microscopy-based chromosome counting assays, PCR analysis, and Bionano optical genome mapping. To evaluate the two clonal lines for common mESC aneuploidies [43], we performed Giemsa staining and subsequent chromosomal counting (**Fig. S10F**), and found the majority of cells had no detectable loss of chromosomes. PCR-based assessment of X and Y chromosomes, showed retention of the Y chromosome (**Fig. S10G**). We also performed comprehensive structural genome analysis using Bionano (**Fig. 4E),** which indicated that all 40 chromosomes were present in each of the cell lines with no apparent aneuploidy, translocations, or other genomic abnormalities. Copy number variants were minimal and often conserved between samples including unedited controls, indicating that these variants were not caused by editing but already existed in the B6129 mouse strain used to derive the mESC line.

The two edited mESC clones demonstrated robust chimera formation, as each produced mice with near full mESC contribution in a single generation via injection into 8-cell stage embryos (**Fig. 5A**). First, we determined that mESCs localize to and form the bulk of the inner cell mass by using a mESC line stably expressing GFP (**Fig. 5B**). Next, we injected mESC clone 25 (Experiment D) and clone 14 (Experiment E) (**Fig. 4D**) into C57BL/6N 8-cell embryos. We observed that 99% (89/90) of the 8-cell stage embryos injected reached the blastocyst stage after two days in culture, suggesting that *in vitro* embryo development was not negatively affected (**Table 4**). Between the two experiments, we generated seven mice edited at rates of 98-100% at each target site (**Fig. 5C**, **Figs. S11A and S11B**). The detailed genotypes of a selected mouse from Experiment D and Experiment E are shown in **Fig. 5D**. Given that all of the mice born were male and their editing profile exactly matched that of the respective donor mESCs, we infer that these mice were nearly 100% ESC derived. Overall, this method produced near fully edited mice with an efficiency of 8% (seven mice from 90 8-cell embryos injected).

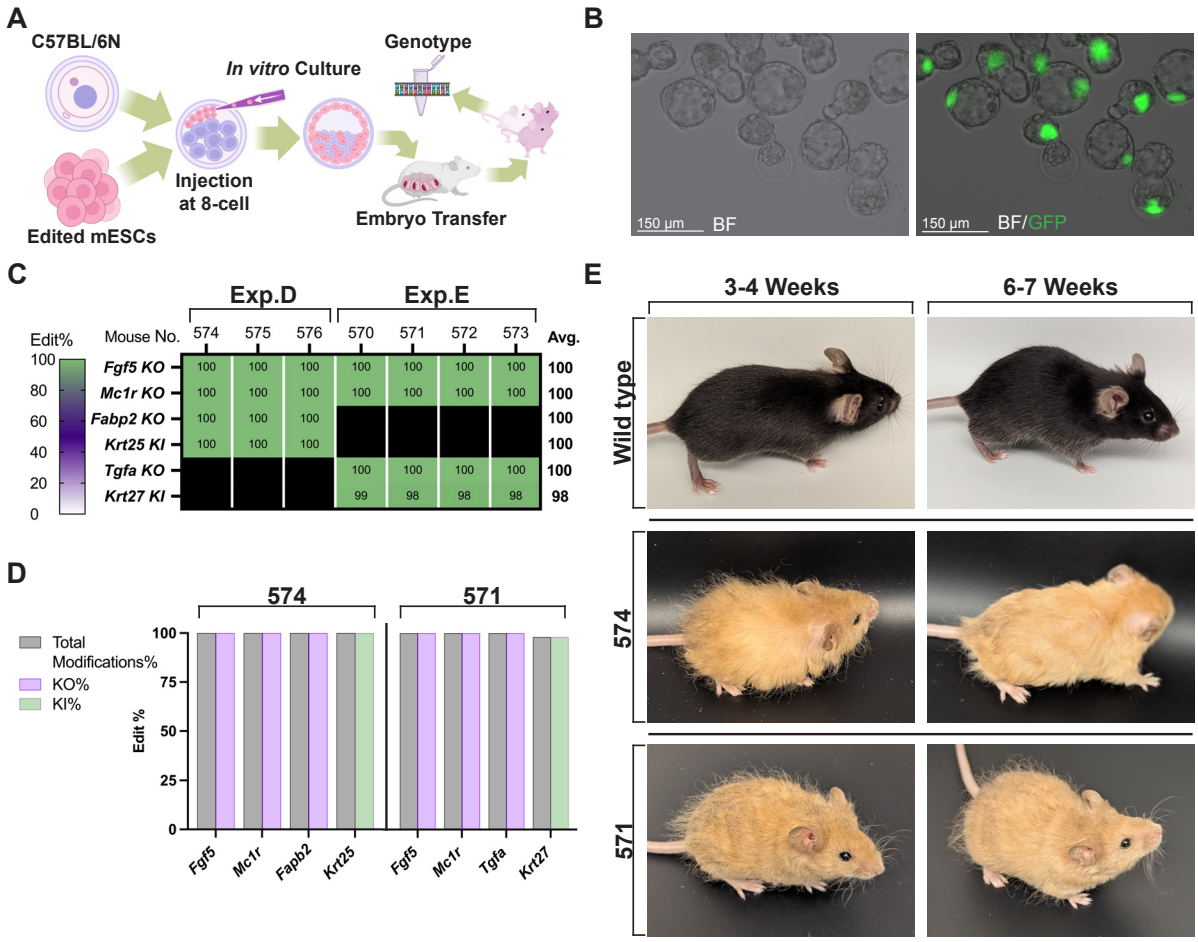

Fig. 5. Experiment D and E: generation of high yield woolly mouse chimeras using CRISPR/Cas9 multiplex edited, monoclonal mouse embryonic stem cells. (A) Workflow for highly efficient production of edited mice within a single generation. We cultured edited monoclonal mouse ESCs in 2i medium and injected eight mESCs into an 8-cell stage C57BL/6N zygote. We cultured the injected embryos in KSOM medium until the blastocyst stage and transferred the embryos to surrogates. Twenty-one days after birth, we collected ear punches for genotyping. **(B)** Representative image of blastocyst-stage embryos injected at the 8-cell stage with mESCs expressing GFP. Images taken at 20X. BF, bright field. **(C)** The KO% and KI% editing profile of mice generated from Experiment D and E monoclonal cell lines. Each column is NGS data from n = 1 mouse. "Mouse No." is the name of the mouse used in this study. **(D)** The total modifications%, KO%, and KI% from mice #574 (Experiment D) and #571 (Experiment E). **(E)** Photos of mouse #574 from Experiment D and mouse #571 from Experiment E at 3-4 weeks old and 6-7 weeks old. Wild-type reference photos are from an age-matched C57BL/6N mouse.

Mice from both Experiments D and E had a gold coat, long guard hairs, and distinctive hair textures (**Fig. 5E**). Mice from Experiment D (*Fgf5, Mc1r, Fabp2* KO; *Krt25* KI) (**Fig. 5E** #574**, Fig. S12**) had a rough, wiry pelage that produced hairs which stuck out from the body. This wiriness smoothed out after six weeks of age, as previously reported for the *Krt25* mutation [23], while the coat sustained altered roughness and length of fur. Mice produced in Experiment E (*Fgf5, Mc1r, Tgfa* KO; *Krt27* KI) (**Fig. 5E** #571**, Fig. S13**) had long disordered guard hairs with a rough texture, as well as wavy awl/auchene/zigzag hairs that remained closer in place to the

body. The mice produced within each experiment were strikingly similar to each other, as expected due to near full derivation from their respective clonal mESC lines.

Table 4. ESC editing animal production summary

Experiment	ES cell line	# Blastocysts developed / # Injected 8-cell embryos (%)	Recipients	# Pups born / # Blastocysts transferred (%)	# Live pups / # Pups born (%)	# Live near 100% chimeras
D	Exp. D, clone 25	58 / 59 (98%)	3	6 / 58 (10%)	3 / 6 (50%)	3
E	Exp. E, clone 14	31 / 31 (100%)	2	5 / 31 (16%)	4 / 5 (80%)	4

Summary

We used several genome editing approaches to generate mice with combinatorial knock-outs or knock-ins in ten genes involved in hair follicle development and lipid metabolism (**Figs. 1A and 1B**). The targeted genes were chosen based on mammoth-specific alleles identified through comparative genomics and hair-associated variants previously characterized in mice. Our genetically modified mice have hair phenotypes including wiry coats, wavy hair, altered hair color, and woolly coats (**Figs. 2H, 3H, 5E, S1C, S1D, S2-S5, S6D, S7-9, S11-13**). Our mouse models provide a resource for future research into hair development pathways and phenotype engineering insight relevant to woolly mammoth de-extinction.

Our optimized protocols and workflows enable the rapid and efficient production of multiplexed mouse models (**Fig. 1B**). Direct zygote editing with CRISPR/Cas9 enabled simultaneous KO of up to five genes with editing efficiencies exceeding 90% (**Figs. 2C, 2E**). Similarly, CBE facilitated precise editing of seven genes simultaneously, and fluorescent protein expression served as an effective reporter of editing success (**Figs. 3D, 3E**). Importantly, these two approaches allow rapid production of edited animals and enable interrogation of phenotypes in a single step. Our last strategy involved a two-step process: first mESCs were edited *in vitro* and fully modified clones were identified; these clones were then injected into 8-cell embryos yielding chimeric pups (**Figs. 4A and 5A**). This approach yielded mice derived almost entirely from mESCs (**Fig. 5C**), dramatically reducing the time needed to produce fully engineered mice and allowing F0 characterization of phenotypes [14–16]. While each of these strategies were successful, any one of these approaches could have been solely engaged to produce our engineered woolly mice.

While mouse models provide an experimentally tractable system for evaluating the functional consequences of genetic modifications, hair follicle biology and physiological parameters probably differ from those of proboscideans, as is the case for humans [44]. Additionally, the mammoth cold-adaptive phenotype would have involved complex physiological modifications beyond hair morphology, including changes in adipose distribution, vascular architecture, and metabolic thermoregulation. Here, we engineered FABP2 to replicate the mammoth variant and found that, in our small sample size, average body mass did not significantly differ between gene-edited and wild-type mice. Future experiments will examine the effect of high fat diets and temperature preferences of our woolly mice and provide deeper understanding of the potential physiological implications of these engineered traits.

Despite these limitations, the multiplexed editing strategies and mouse models established here provide a foundation for evaluating complex combinations of genetic modifications leading to the mammoth phenotype. Future work will evaluate additional mammoth-specific variants associated with other cold-adaptive traits. Findings from these experiments will continue to inform prioritization of genetic modifications for elephant cell engineering and mammoth de-extinction. The technical advances in multiplexed editing demonstrated here also have implications for both basic research and therapeutic applications requiring precise orchestration of multiple genetic modifications.

Acknowledgements

The authors would like to thank Dr. Robert Hammer, John Ritter and the Transgenic Core at UTSW for their insight and support providing custom mouse model services. We would also like to thank Faith McCorkle, Katie SoRelle and Deb McWilliams of the Colossal animal care team, and the staff at the Animal Resource Center at UTSW for their excellent care. We would like to thank Gregory Knox for reagent preparation. Finally, we would like to thank Dr. Daniel Rokhsar, Dr. Andrew Pask, and Dr. Jun Wu for reviewing this work and for helpful comments on this manuscript.

Competing Interests

The authors have filed a patent application based on the results of this work. All authors are current or former employees, or scientific advisors/consultants for Colossal Biosciences and/or Form Bio, and may hold stock and/or stock options in these companies. G.C. is a founder and shareholder of Colossal Biosciences and others - full disclosure for G.C. is available at http://arep.med.harvard.edu/gmc/tech.html.

Author Contributions

Conceived and designed the experiments, performed experiments, carried out data analysis: R.C., K.S., M.C., R.V.S., R.W., R.G., J.W., A.L., J.B., J.S., and M.A.

Cell culture and molecular biology experiments: R.C., M.C., R.W., R.G., J.W., J.B., J.S., and R.O.

Embryology experiments: K.S., R.V.S., A.L., and Y.Q.

Animal work: R.W., K.S., J.K., and M.J.

Bionano data acquisition and analysis: A.M.IV

NGS data acquisition: C.C., J.P., and A.M.IV

Bioinformatics analysis: K.B., J.M., M.M., J.W., and B.C.

Writing: R.C., K.S., M.C., R.V.S., R.W., R.G., J.W., A.L., J.B., J.S., B.S., and M.A.

Project supervision: A.B., B.C., M.J., J.K., B.L., G.C., B.S., and M.A.

Project conceptualization: B.L., G.C., B.S., L.D., T.v.d.V., and M.A.

Funding acquisition: B.L.

All authors were involved in reviewing and revising the manuscript.

Materials and Methods

Guide RNA and HDR donor design

For Cas9 editing, we designed most synthetic single-guide RNA (sgRNA) using the CRISPR Predict tool in Geneious Prime (Geneious, 2024.0.7) and others we manually designed. We assessed guide sites for CRISPR activity using established efficiency scores [45]. We evaluated off-target effects against selected regions of interest and the entire *Mus musculus* genome, GRCm39, with a tolerance of up to 3 mismatches. We further evaluated potential off-target edits in the Integrated DNA Technologies (IDT) CRISPR-Cas9 guide RNA design checker (IDT, IA, USA). We designed ssODN templates for HDR symmetrically around the cut site disrupted by the sgRNA. We used homology arms of thirty, forty, and sixty base pairs and PAM silencing mutations for some donors.

For cytosine base editing (CBE), we designed sgRNAs to target regions where the C-to-T conversion would either introduce a premature stop codon [40] or disrupt a splice site [41], both resulting in gene disruption and loss of function. The editing designs in this study ensured that any C-to-T bystander effect from CBE would not impede stop codon introduction or splice site mutation. However, edits other than C-to-T [46], although less frequent, could abolish the effect of the intended point mutation. Unintended edits were considered and evaluated during guide design and genotyping.

The sequences of all sgRNA and HDR donors used in this study are listed in **Tables S3 and S4**.

Plasmids and *in vitro* transcription

We cloned an *in vitro* transcription plasmid template via NEBuilder HiFi DNA Assembly (New England Biolabs (NEB), MA, USA). This vector comprised a T7 promoter to initiate transcription, CBE, mScarlet3, and flanking UTR sequences. Correct assembly was verified using Oxford Nanopore sequencing (Plasmidsaurus, OR, USA).

We generated a linear DNA amplicon that included the T7 promoter, coding regions, and UTRs using KOD One (Sigma-Aldrich, MO, USA). We performed gel electrophoresis and excised the band corresponding to the amplicon, which we gel purified using the QIAquick Gel Extraction Kit (Qiagen, MD, USA). We then bead purified the eluted DNA using AMPure XP Beads (Beckman Coulter, CA, USA).

The purified amplicon served as a template for an *in vitro* transcription reaction using the HiScribe® T7 High Yield RNA Synthesis Kit (NEB, MA, USA). We incubated the reaction at

37°C for 2 hours, and then purified mRNA using the Monarch RNA Cleanup Kit (NEB, MA, USA). We measured the yield and purity of the mRNA using a Denovix DS-11 (Denovix Inc, DE, USA) and aliquoted purified mRNA, which we stored at -80°C until use.

Animal housing and strains

Animal work described in this manuscript was approved and conducted under the oversight of the UT Southwestern Institutional Animal Care and Use Committee (IACUC) Dallas, TX, USA. All mice were housed in standard cages within a specific pathogen-free facility, maintained under a 12-hour light/dark cycle.

We used B6SJLF1 (The Jackson Laboratory, ME, USA) mice for zygote editing (Experiment A-C) and C57BL/6N (Charles River Laboratories, MA, USA) mice as embryo donors for chimera generation (Experiment D-E). ICR (Inotiv, IN, USA) mice served as pseudopregnant recipients. We obtained frozen B6C3F1 × B6D2F1 embryos from Embryotech (MA, USA).

Pronuclear embryo production

We superovulated female B6SJLF1 mice (8–12 weeks old) by administering 7.5 IU of pregnant mare serum gonadotropin (PMSG; Prospec, Rehovot, Israel), followed 48 hours later by 7.5 IU of human chorionic gonadotropin (hCG; Sigma-Aldrich, MO, USA). These females were then mated with male B6SJLF1 mice and fertilized embryos were collected from the oviducts 20 hours after the hCG injection. We maintained the harvested embryos in KSOM medium (EmbryoMax® Advanced KSOM Embryo Medium, Sigma-Aldrich, MO, USA). We obtained fertilized oocytes from C57BL/6N mice following the superovulation and mating protocol described above, except with 6.0 IU of PMSG followed by 6.0 IU hCG.

We thawed frozen B6C3F1 × B6D2F1 zygotes (Embryotech, MA, USA) at room temperature for 2 minutes, followed by washing and incubation in KSOM medium for 10 minutes at room temperature. We then cultured the zygotes in KSOM medium under mineral oil (Sigma-Aldrich, MO, USA) at 37°C in an atmosphere of 5% CO_2, 5% O_2, and 90% N_2 for one hour before proceeding with further experiments.

Zygote electroporation and pronuclear injection

We prepared RNP complexes for electroporation by mixing recombinant *S. pyogenes* Cas9 nuclease (Alt-R® S.p. HiFi Cas9 Nuclease V3, IDT, IA, USA), sgRNA (Synthego, CA, USA or IDT, IA, USA), and Alt-R® Cas9 Electroporation Enhancer (IDT, IA, USA) in OPTI-MEM®

medium (Gibco, NY, USA). The concentrations of each component are provided in **Table S5**. We placed zygotes (30–50) into a 0.1 cm-gap electroporation cuvette (Bio-Rad, CA, USA) containing 10 µL of RNP complexes and performed electroporation at room temperature using an ECM 2001 Electroporation System (BTX, MA, USA) with the following parameters: 30 V direct current, 3 ms pulse duration, and 5 pulses.

For pronuclear injection, we prepared a solution containing CBE mRNA and sgRNA (Synthego, CA, USA or IDT, IA, USA) using nuclease-free water (Synthego, CA, USA). The concentrations of CBE mRNA and sgRNA are listed in **Table S6**. We injected this solution into the pronuclei of zygotes placed in droplets of KSOM medium under mineral oil. We performed microinjections using a FemtoJet 4i microinjector (Eppendorf, Hamburg, Germany) and a Nikon ECLIPSE Ti2 inverted microscope (Nikon, Tokyo, Japan) equipped with micromanipulators (Narishige, Ibaraki, Japan).

After electroporation and pronuclear injection, we cultured embryos in KSOM medium under mineral oil at 37°C in an atmosphere of 5% CO_2, 5% O_2, and 90% N_2 for 4 days. We then transferred blastocyst-stage embryos into the uteri of pseudopregnant ICR mice at 2.5 days post coitum.

Fluorescent imaging

We imaged fluorescent blastocysts injected with CBE-mScarlet3 mRNA or injected with mESC expressing GFP using the Invitrogen EVOS M7000 Imaging system (Thermo Fisher Scientific, MA, USA) equipped with a 20X objective lens and RFP and GFP LED cubes.

Murine embryonic stem cell (mESC) derivation

We derived mESCs from hybrid F1-fertilized embryos generated by crossing C57BL/6J females with 129/S4 males. We collected one-cell zygotes from plugged females following treatment with PMSG (Prospec, Rehovot, Israel) and hCG (Sigma-Aldrich, MO, USA), which we then cultured in advanced KSOM medium (Sigma-Aldrich, MO, USA) until reaching the blastocyst stage at four days post-fertilization. We removed the zona pellucida from the blastocysts via brief exposure to Tyrode's acidic solution (Sigma-Aldrich, MO, USA). Zona-free blastocysts were collected using a mouth pipette, washed three times in KSOM medium, and individually plated in 48-well plates containing inactivated mouse embryonic fibroblasts (iMEFs, Thermo Fisher Scientific, MA, USA) and ESC derivation medium. The ESC derivation medium consisted of Knockout Dulbecco’s Modified Eagle Medium (KO-DMEM, Gibco, MA, USA) supplemented with 20% Knockout Serum Replacement (KOSR, Gibco, MA, USA), recombinant

mouse leukemia inhibitory factor (LIF, Sigma-Aldrich, MO, USA), L-glutamine (Sigma-Aldrich, MO, USA), penicillin/streptomycin (Sigma-Aldrich, MO, USA), non-essential amino acids (Sigma-Aldrich, MO, USA), and β-mercaptoethanol (Sigma-Aldrich, MO, USA). After 7–8 days of culture, blastocyst outgrowths were enzymatically dissociated using 0.025% trypsin solution (Sigma-Aldrich, MO, USA) for 10 minutes. We neutralized the trypsinization reaction with ESC culture medium and the cells were then seeded onto 24-well plates pre-coated with iMEFs. We subsequently expanded several ESC colonies to 6-well plates on iMEFs for further use. We characterized ESC clonal lines for genomic stability, and selected a fully normal male line at passage 2 for use in this study.

mESC Culture

We maintained B6129 ESCs on DR4 iMEFs at 37°C with 5% CO_2 in culture medium consisting of KO-DMEM (Gibco, MA, USA) supplemented with 15% KOSR (Gibco, MA, USA), 1% GlutaMAX (Gibco, MA, USA), 1% MEM Non-Essential Amino Acids (Gibco, MA, USA), 100 uM 2-Mercaptoethanol (Gibco, MA, USA), 1000 U/mL LIF (Sigma-Aldrich, MO, USA), and 1% penicillin/streptomycin (Gibco, MA, USA), changing the growth medium daily. We used collagenase (Gibco, MA, USA) to gently lift ESCs from the iMEF feeder layer, followed by a brief incubation in diluted Accumax (Thermo Fisher Scientific, MA, CA) to generate a single cell suspension for passaging and electroporation.

Transfection of mESC cell lines

We formed RNP complexes by combining 3200 ng of *S. pyogenes* Cas9 nuclease (Alt-R® S.p. HiFi Cas9 Nuclease V3, IDT, IA, US), 400 pmol of sgRNA (Synthego, CA, USA or IDT, IA, USA), and 5 µL of Alt-R® Cas9 Electroporation Enhancer (IDT, IA, USA). For RNPs targeting HDR, we mixed an additional 400 pmol of single-stranded DNA oligos (IDT, IA, USA) and 5 µL of Alt-R® Cas9 Electroporation Enhancer (IDT, IA, USA) with Cas9 and sgRNA. Complexes were allowed to form for 10-20 minutes at room temperature.

We electroporated mESCs with the Lonza P3 Primary Cell 4D-Nucleofector X Kit L (Lonza, Basel, Switzerland) using program CG104, according to the manufacturer's protocol. Post electroporation, we seeded mESCs back on DR4 iMEFs in growth medium supplemented with Y-27632 2HCL (Selleckem, TX, USA). For HDR experiments, we added 1 µM of Alt-R®HDR enhancer (IDT, IA, USA) to the medium.

Clonal isolation of edited mESC lines

After three serial rounds of electroporation as described above, we single-cell sorted mESCs directly onto a 96-well plate pre-coated with iMEFs using the SONY SH800S sorter equipped with a 100 μM chip (SONY, CA, USA). We then expanded mESC colonies to a 24-well plate pre-coated with DR4 iMEFs until approaching confluency. Ten percent of the mESCs were collected for Sanger sequencing. The remaining ESCs were either cryopreserved in 90% KOSR/10% DMSO or seeded on laminin-coated plates (Laminin-511, BioLamina, Sundyberg, Sweden) for downstream analysis. Selected mESC clones for animal generation were thawed and expanded ten days before embryonic injection.

Detection of Y chromosome by PCR

We performed PCR on mESC clonal expansions to detect loss of the Y chromosome following established primer designs [47]. We used a chromosomally normal male B6129 ESC line with an intact Y chromosome as a positive control and a male B6129 ESC line with known Y chromosome loss as a negative control. We performed a 15 μl PCR using KOD ONE (Sigma-Aldrich, MO, USA) as follows: 38-40 cycles of 98°C for 15 seconds, 60°C for 5 seconds, and 68°C for 5 seconds. We ran 10 μl of the resulting product on a 2% agarose gel at 220 volts for 30 minutes, and obtained a gel image using the iBright. (Thermo Fisher Scientific, MA, USA). Assuming no loss of the Y, the result should be a Y-chromosome specific amplicon (280 bp) and two amplicons specific to the X chromosome (685 bp and 480 bp).

Chromosome counting assay

We performed chromosome counting of mESCs as previously described [48,49]. Briefly, we seeded clonal mESC populations onto feeder-free laminin-coated (BioLamina, Sundyberg, Sweden) tissue culture plates and maintained the cells in culture medium until cells reached confluency. We then added 200 ng/mL colchicine (Sigma-Aldrich, MO, USA) to the culture medium and incubated cells at 37°C for 3 hours. Following the incubation, we detached cells from the plate with 1:2 diluted Accumax (Thermo Fisher Scientific, MA, USA) and prepared a single-cell suspension by pipetting. We then pelleted the cells via centrifugation and subsequently resuspended the cells in 75 mM KC. Following an incubation at 37°C for 8 minutes, we fixed cell suspensions in a 3:1 (v/v) solution of methanol and glacial acetic acid (Sigma-Aldrich, MO, USA) at room temperature. Fixed cells were dropped onto glass slides and stained with KaryoMAX Giemsa stain (ThermoFisher, MA, USA) in Gurr buffer (Gibco, MA,

USA). We imaged stained cells using bright-field microscopy (EVOS M7000) and counted chromosomes using the particle analysis tool in the ImageJ software (v1.54f).

Bionano analysis

We performed bionano analysis of mESCs according to manufacturer specifications. Briefly, we pelletted 500K to 1M mESCs and isolated ultra high molecular weight (UHMW) genomic DNA as described in the Bionano Prep SP-G2 Fresh Cell Pellet DNA Isolation Protocol (Bionano, Doc no. CG003). We then fluorescently labeled UHMW gDNA by the Direct Label Enzyme (DLE-1) and then stained for backbone visualization (Bionano Prep Direct Label and Stain (DLS) Protocol, Doc no. 30206). We loaded the labeled and stained UHMW gDNA sample onto a Saphyr Chip and into the Saphyr System Instrument (Bionano Saphyr System User Guide, Doc no. 30247) and used Bionano Solve identify structural variations (SV) and low variant allele fraction variants (VAF) (Bionano Solve Theory of Operation: Structural Variant Calling, Doc no. CG-30110). We analyzed unedited mESCs in parallel as the background to extract SV information for edited cell lines. The resolution for detecting variants with this method is ~500bp.

Chimera production

We maintained mESCs in the ground state of pluripotency for up to three passages in N2B27 basal medium, modified from a previous publication [50], seven days before 8-cell stage injection. The medium comprised of a 1:1 mixture of DMEM/F12 (Gibco, MA, USA) and Neurobasal (Gibco, MA, USA), supplemented with 1% (v/v) B-27 (Gibco, MA, USA), 0.5% (v/v) N-2 (Gibco, MA, USA), 1% (v/v) GlutaMAX (Gibco, MA, USA), 2 mM MEM Non-Essential Amino Acids (Gibco, MA, USA), 100 U/mL Penicillin-Streptomycin (Sigma-Aldrich, MO, USA), and 0.1 mM 2-mercaptoethanol (Sigma-Aldrich, MO, USA). Following Ying et al. 2008 [51], we further supplemented the medium with 1000 U/mL human LIF (Sigma-Aldrich, MO, USA) and the inhibitors 1 μM CHIR99021 (Selleckchem, TX, USA) and 0.4 μM PD0325901 (Selleckchem, TX, USA).

We produced chimeras by adapting the previously described laser-assisted protocol [52]. We cultured zygotes from C57BL/6N mice in KSOM medium (Millipore, MA, USA) for approximately 48 hours at 37°C under 5% CO_2 and 5% O_2. We selected embryos at the 8-cell stage, before compaction, for manipulation. Using a holding pipette with 10-15 μm ID (Sunlight Medical, FL, USA) to stabilize the embryos, we made a perforation in the zona pellucida (ZP) with an 800 ms tangential laser pulse (100% power) from an XYClone laser system (Hamilton

Thorne Bioscience, MA, USA), targeting the outer margin of the ZP in a region away from blastomeres. We injected eight mESCs into the perivitelline space using an injection pipette with 15 µm ID (Sunlight Medical, FL, USA). Following injection, we washed the embryos and cultured them in KSOM under the same environmental conditions. Embryos that developed into blastocysts were collected and transferred to the uterine horns of pseudopregnant mice.

Genotyping

To collect samples for genotyping, we harvested embryos at the blastocyst stage, collected mESCs from single-cell Accumax (Thermo Fisher Scientific, MA, CA) suspensions, and obtained ear notch samples from individual mice 21–26 days after birth. We lysed each sample with Quick Extract (Fisher Scientific Company, NH, USA) and placed each in a thermocycler at 65°C for 15 minutes followed by 98°C for 2 minutes.

We amplified genomic regions spanning the mutation of interest via PCR, followed by next generation sequencing (NGS) or Sanger sequencing as described below. All primer sequences used for genotyping are listed in **Table S7** and were designed in Geneious Prime (Geneious, 2024.0.7).

To prepare amplicons for NGS genotyping, we performed two step PCR. PCR1 used KOD ONE (Sigma-Aldrich, MO, USA) and a thermocycle consisting of 30-35 cycles of 98°C for 15 seconds, 60°C for 5 seconds, and 68°C for 5 seconds. We added 1 µl of PCR1 into the PCR2 mixture that included custom indexes for i5 and i7 adapter sequences (IDT, IA, USA). The PCR2 thermocycle consisted of 8 cycles of 98°C for 15 seconds, 60°C for 5 seconds, and 68°C for 5 seconds. We confirmed amplification via gel electrophoresis with 5 µl of PCR2.

Next, we pooled PCR2 samples into a purified library pool using AMPure XP Beads (Beckman Coulter, CA, USA), and quantified DNA concentration by both Qubit Flex Fluorometer (Thermo Fisher Scientific, MA, USA) and a D1000 ScreenTape (Agilent Technologies, CA, USA) on the Agilent TapeStation. We sequenced libraries using either a 300- or 500-cycle kit on the Illumina MiSeq or the NextSeq2000 instruments (Illumina, CA, USA) targeting ten thousand reads per sample. We uploaded the data onto the Form Bio (Form Bio Inc., TX, USA) platform and ran the VALID workflow. Briefly, sequence read pairs are merged using fastp [53], then reads are aligned to the expected amplicons using Magic-blast [54] for edited and wild-type cells. We used these alignments to calculate editing efficiencies and identify off-target edits overlapping the amplicon region.

For Sanger sequencing, we performed 15 µl PCRs using KOD ONE (Sigma-Aldrich, MO, USA) as follows: 38-40 cycles of 98°C for 15 seconds, 60°C for 5 seconds, and 68°C for 5

seconds. After PCR was complete, we ran 5 µl of the samples on a 2% agarose gel for 30 minutes to confirm presence of a band. We sent the remaining 10 µl of the unpurified PCR to Genewiz/Azenta (Genewiz/Azenta, NJ, USA) for Sanger sequencing. We ran ab1 files from Sanger sequencing on the Synthego website for ICE Analysis.

We define gene knock-out (KO) as exonic insertions or deletions (indels) not in multiples of three, an exonic indel over 100 bp, introduction of a stop codon, or a splice site mutation. For large indels that may influence the mapping of NGS reads (usually >100 bp), we used electrophoresis band patterning and Sanger sequencing to confirm absence of wild-type sequences. All mice were genotyped primarily by NGS and supplemented by Sanger sequencing.

Whole genome sequencing and off-target analysis

For each sample, we extracted genomic DNA using the NucleoSpin Tissue kit following manufacturer instructions (Macherey-Nagel, Düren, Germany). Libraries were prepared using the Illumina DNA Prep kit (Illumina, CA, USA). We used double-sided bead purification to purify amplified libraries which we quantified using an Agilent TapeStation (Agilent Technologies, CA, USA) prior to normalization and pooling. Libraries were then sequenced on the NextSeq2000 (Illumina, CA, USA) using XLEAP-SBS chemistry targeting 30x genomic coverage per sample.

We identified editing at off-target sites by whole genome sequencing and alignment. We used the Valid WGS workflow on the Form Bio platform to identify SNVs, indels, and structural variants to identify edits. In this workflow, we trimmed reads using fastp and then aligned them to the mm39 reference genome [55] using Sentieon optimized BWA MEM [56,57]. Duplicate reads were marked using Picard MarkDuplicates. Somatic variants were detected using the Sentieon TNHaplotyper2 tool while structural variant calls were detected using DNAscope. We filtered variants based on multiple filtering criteria (Strand bias, Alternate Allele Count < 2, Variant Allele Frequency < 0.7) to predict on and off target edits. After filtering, on target and off target variants list were split based on the intended location of on targets. Quality reports were produced by MultiQC. Variant effects were determined using snpEff.

For zygote editing, we took a targeted approach to determine off-target editing to account for normal genetic variations between individuals. We predicted off-target binding sites for all multiplexed guides in each zygote-editing experiment using the Form Bio platform (Formbio, Texas, USA) via the DR GENE workflow, which uses an in-house implementation of the runCrisprBwa function from the crisprVerse package in R [58]. All predicted off-target sites with three or fewer mismatches to the sgRNA protospacers were interrogated for off-target

editing from the WGS data. For mice produced from CBE-edited zygotes, variants found within ±20bp of a predicted off-target binding site were considered off-target edits. To account for larger potential alterations due to NHEJ in the mice produced from Cas9-edited zygotes, variants found within ±200bp of a predicted off-target binding site were considered off-target edits. Of these, all variants with a VAF greater than 0.7 and read depth greater than 5 are reported. As ESC and ESC derived samples originate from the same B6129 ESC cell line, we report all off-target variants with a variant allele frequency (VAF) greater than 0.7 and read depth greater than 5.

References

1. Vartanyan, S. L., Arslanov, K. A., Karhu, J. A., Possnert, G. & Sulerzhitsky, L. D. Collection of radiocarbon dates on the mammoths (*Mammuthus Primigenius*) and other genera of Wrangel Island, northeast Siberia, Russia. *Quat. Res.* **70**, 51–59 (2008).
2. Dehasque, M. *et al.* Temporal dynamics of woolly mammoth genome erosion prior to extinction. *Cell* **187**, 3531-3540.e13 (2024).
3. Shapiro, B. Pathways to de-extinction: how close can we get to resurrection of an extinct species? *Funct. Ecol.* **31**, 996–1002 (2017).
4. Díez-Del-Molino, D. *et al.* Genomics of adaptive evolution in the woolly mammoth. *Curr. Biol. CB* **33**, 1753-1764.e4 (2023).
5. Tschaharganeh, D. F., Lowe, S. W., Garippa, R. J. & Livshits, G. Using CRISPR/Cas to study gene function and model disease in vivo. *FEBS J.* **283**, 3194–3203 (2016).
6. Zuo, E. *et al.* One-step generation of complete gene knockout mice and monkeys by CRISPR/Cas9-mediated gene editing with multiple sgRNAs. *Cell Res.* **27**, 933–945 (2017).
7. Teixeira, M. *et al.* Electroporation of mice zygotes with dual guide RNA/Cas9 complexes for simple and efficient cloning-free genome editing. *Sci. Rep.* **8**, 474 (2018).
8. Wang, H. *et al.* One-step generation of mice carrying mutations in multiple genes by CRISPR/Cas-mediated genome engineering. *Cell* **153**, 910–918 (2013).
9. Williams, A., Henao-Mejia, J. & Flavell, R. A. Editing the Mouse Genome Using the CRISPR-Cas9 System. *Cold Spring Harb. Protoc.* **2016**, pdb.top087536 (2016).
10. Cong, L. *et al.* Multiplex genome engineering using CRISPR/Cas systems. *Science* **339**, 819–823 (2013).
11. Komor, A. C., Kim, Y. B., Packer, M. S., Zuris, J. A. & Liu, D. R. Programmable editing of a target base in genomic DNA without double-stranded DNA cleavage. *Nature* **533**, 420–424 (2016).
12. Gaudelli, N. M. *et al.* Programmable base editing of A•T to G•C in genomic DNA without DNA cleavage. *Nature* **551**, 464–471 (2017).
13. Anzalone, A. V. *et al.* Search-and-replace genome editing without double-strand breaks or donor DNA. *Nature* **576**, 149–157 (2019).
14. Ukai, H., Kiyonari, H. & Ueda, H. R. Production of knock-in mice in a single generation from embryonic stem cells. *Nat. Protoc.* **12**, 2513–2530 (2017).
15. Sumiyama, K. *et al.* Easy and efficient production of completely embryonic-stem-cell-derived mice using a micro-aggregation device. *PloS One* **13**, e0203056 (2018).
16. Funano, S., Tone, D., Ukai, H., Ueda, H. R. & Tanaka, Y. Rapid and easy-to-use ES cell

manipulation device with a small groove near culturing wells. *BMC Res. Notes* **13**, 453 (2020).
17. Brennan, B. M. *et al.* The mouse wellhaarig (we) mutations result from defects in epidermal-type transglutaminase 3 (Tgm3). *Mol. Genet. Metab.* **116**, 187–191 (2015).
18. Guo, N., Hawkins, C. & Nathans, J. Frizzled6 controls hair patterning in mice. *Proc. Natl. Acad. Sci.* **101**, 9277–9281 (2004).
19. Chang, H., Cahill, H., Smallwood, P. M., Wang, Y. & Nathans, J. Identification of Astrotactin2 as a Genetic Modifier That Regulates the Global Orientation of Mammalian Hair Follicles. *PLoS Genet.* **11**, e1005532 (2015).
20. Radden, L. A. *et al.* The wooly mutation (wly) on mouse chromosome 11 is associated with a genetic defect in Fam83g. *BMC Res. Notes* **6**, 189 (2013).
21. Hébert, J. M., Rosenquist, T., Götz, J. & Martin, G. R. FGF5 as a regulator of the hair growth cycle: evidence from targeted and spontaneous mutations. *Cell* **78**, 1017–1025 (1994).
22. Mann, G. B. *et al.* Mice with a null mutation of the TGFα gene have abnormal skin architecture, wavy hair, and curly whiskers and often develop corneal inflammation. *Cell* **73**, 249–261 (1993).
23. Du, X., Li, X., Smart, N. G. & Beutler, B. Mutagenetix 'Plush'. *MUTAGENETIX* https://mutagenetix.utsouthwestern.edu/phenotypic/phenotypic_rec.cfm?pk=96 (2011).
24. MGI Krt27. https://www.informatics.jax.org/allele/MGI:3522000 (2005).
25. Robbins, L. Pigmentation phenotypes of variant extension locus alleles result from point mutations that alter MSH receptor function. *Cell* **72**, 827–834 (1993).
26. van der Valk, T. *et al.* Million-year-old DNA sheds light on the genomic history of mammoths. *Nature* **591**, 265–269 (2021).
27. Huang, X., Zhou, Y., Sun, Y. & Wang, Q. Intestinal fatty acid binding protein: A rising therapeutic target in lipid metabolism. *Prog. Lipid Res.* **87**, 101178 (2022).
28. Agellon, L. B. *et al.* Loss of intestinal fatty acid binding protein increases the susceptibility of male mice to high fat diet-induced fatty liver. *Biochim. Biophys. Acta BBA - Mol. Cell Biol. Lipids* **1771**, 1283–1288 (2007).
29. Chen, Y. & Agellon, L. B. Distinct Alteration of Gene Expression Programs in the Small Intestine of Male and Female Mice in Response to Ablation of Intestinal Fabp Genes. *Genes* **11**, 943 (2020).
30. Fontaine, D. A. & Davis, D. B. Attention to Background Strain Is Essential for Metabolic Research: C57BL/6 and the International Knockout Mouse Consortium. *Diabetes* **65**, 25–33

(2016).
31. 000686 - SJL Strain Details. https://www.jax.org/strain/000686.
32. Brilliant, M. H. The mouse p (pink-eyed dilution) and human P genes, oculocutaneous albinism type 2 (OCA2), and melanosomal pH. *Pigment Cell Res.* **14**, 86–93 (2001).
33. Shoji, H. *et al.* A nonsense nucleotide substitution in the oculocutaneous albinism II gene underlies the original pink-eyed dilution allele (Oca2p) in mice. *Exp. Anim.* **64**, 171–179 (2015).
34. Fur, N. L., Kelsall, S. R. & Mintz, B. Base Substitution at Different Alternative Splice Donor Sites of the Tyrosinase Gene in Murine Albinism. *Genomics* **37**, 245–248 (1996).
35. Silvers, W. K. The Agouti and Extension Series of Alleles, Umbrous, and Sable. in *The Coat Colors of Mice: A Model for Mammalian Gene Action and Interaction* (ed. Silvers, W. K.) 6–44 (Springer, New York, NY, 1979). doi:10.1007/978-1-4612-6164-3_2.
36. Ollmann, M. M., Lamoreux, M. L., Wilson, B. D. & Barsh, G. S. Interaction of Agouti protein with the melanocortin 1 receptor in vitro and in vivo. *Genes Dev.* **12**, 316–330 (1998).
37. Wolf Horrell, E. M., Boulanger, M. C. & D'Orazio, J. A. Melanocortin 1 Receptor: Structure, Function, and Regulation. *Front. Genet.* **7**, (2016).
38. Benned-Jensen, T., Mokrosinski, J. & Rosenkilde, M. M. The E92K Melanocortin 1 Receptor Mutant Induces cAMP Production and Arrestin Recruitment but Not ERK Activity Indicating Biased Constitutive Signaling. *PLoS ONE* **6**, e24644 (2011).
39. Jeong, Y. K., Song, B. & Bae, S. Current Status and Challenges of DNA Base Editing Tools. *Mol. Ther. J. Am. Soc. Gene Ther.* **28**, 1938–1952 (2020).
40. Kuscu, C. *et al.* CRISPR-STOP: gene silencing through base-editing-induced nonsense mutations. *Nat. Methods* **14**, 710–712 (2017).
41. Kluesner, M. G. *et al.* CRISPR-Cas9 cytidine and adenosine base editing of splice-sites mediates highly-efficient disruption of proteins in primary and immortalized cells. *Nat. Commun.* **12**, 2437 (2021).
42. Hibshman, G. N. *et al.* Unraveling the mechanisms of PAMless DNA interrogation by SpRY-Cas9. *Nat. Commun.* **15**, 3663 (2024).
43. Gaztelumendi, N. & Nogués, C. Chromosome Instability in mouse Embryonic Stem Cells. *Sci. Rep.* **4**, 5324 (2014).
44. Castro, A. R., Portinha, C. & Logarinho, E. The Emergent Power of Human Cellular vs Mouse Models in Translational Hair Research. *Stem Cells Transl. Med.* **11**, 1021–1028 (2022).
45. Doench, J. G. *et al.* Optimized sgRNA design to maximize activity and minimize off-target

effects of CRISPR-Cas9. *Nat. Biotechnol.* **34**, 184–191 (2016).
46. Neugebauer, M. E. *et al.* Evolution of an adenine base editor into a small, efficient cytosine base editor with low off-target activity. *Nat. Biotechnol.* **41**, 673–685 (2023).
47. McFarlane, L., Truong, V., Palmer, J. S. & Wilhelm, D. Novel PCR assay for determining the genetic sex of mice. *Sex. Dev. Genet. Mol. Biol. Evol. Endocrinol. Embryol. Pathol. Sex Determ. Differ.* **7**, 207–211 (2013).
48. Hwang, S. M. *et al.* The application of an in situ karyotyping technique for mesenchymal stromal cells: a validation and comparison study with classical G-banding. *Exp. Mol. Med.* **45**, e68 (2013).
49. Borgonovo, T., Vaz, I. M., Senegaglia, A. C., Rebelatto, C. L. K. & Brofman, P. R. S. Genetic evaluation of mesenchymal stem cells by G-banded karyotyping in a Cell Technology Center. *Rev. Bras. Hematol. E Hemoter.* **36**, 202–207 (2014).
50. Wu, J. *et al.* An alternative pluripotent state confers interspecies chimaeric competency. *Nature* **521**, 316–321 (2015).
51. Ying, Q.-L. *et al.* The ground state of embryonic stem cell self-renewal. *Nature* **453**, 519–523 (2008).
52. Poueymirou, W. T. *et al.* F0 generation mice fully derived from gene-targeted embryonic stem cells allowing immediate phenotypic analyses. *Nat. Biotechnol.* **25**, 91–99 (2007).
53. Chen, S., Zhou, Y., Chen, Y. & Gu, J. fastp: an ultra-fast all-in-one FASTQ preprocessor. *Bioinformatics* **34**, i884–i890 (2018).
54. Boratyn, G. M., Thierry-Mieg, J., Thierry-Mieg, D., Busby, B. & Madden, T. L. Magic-BLAST, an accurate RNA-seq aligner for long and short reads. *BMC Bioinformatics* **20**, 405 (2019).
55. Genome assembly GRCm39. https://www.ncbi.nlm.nih.gov/datasets/genome/GCF_000001635.27/ (2020).
56. Li, H. Aligning sequence reads, clone sequences and assembly contigs with BWA-MEM. Preprint at https://doi.org/10.48550/ARXIV.1303.3997 (2013).
57. Freed, D., Aldana, R., Weber, J. A. & Edwards, J. S. The Sentieon Genomics Tools - A fast and accurate solution to variant calling from next-generation sequence data. Preprint at https://doi.org/10.1101/115717 (2017).
58. Hoberecht, L., Perampalam, P., Lun, A. & Fortin, J.-P. A comprehensive Bioconductor ecosystem for the design of CRISPR guide RNAs across nucleases and technologies. *Nat. Commun.* **13**, 6568 (2022).

Supplement Figures

Fig. S1

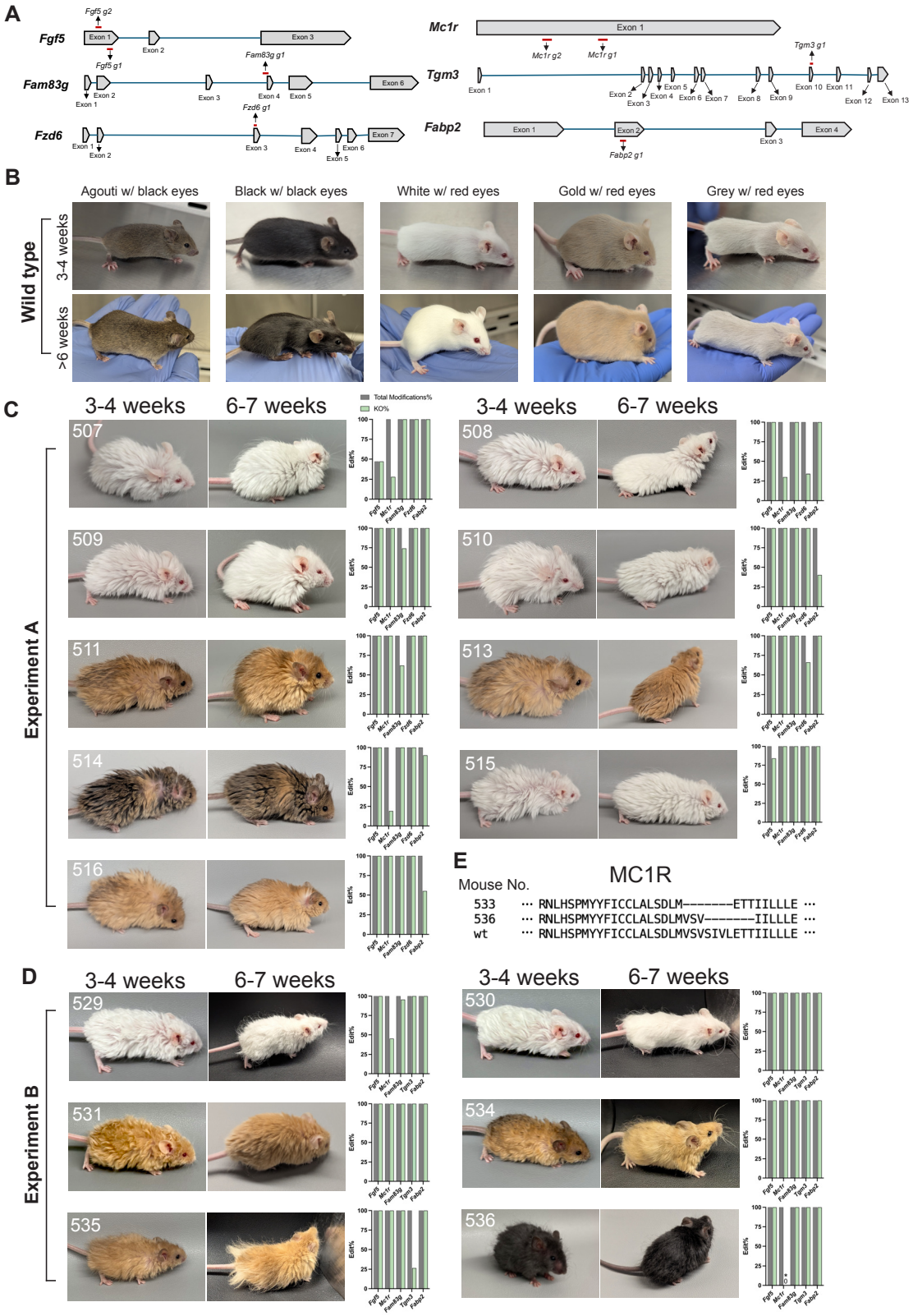

Fig. S1. (A) Target genes and the location of their sgRNAs chosen for Cas9 KO animal production. We selected production sgRNA according to editing efficiency, off-target prediction, and the location of the edit. The ideal edit location should either mimic the previous literature or be in an early exon to facilitate KO. **(B)** Wild-type B6SJL F2 mice (B6 × SJL)F1 × (B6 × SJL)F1 have a variety of coat+eye color combinations: agouti with black eyes (the most common), black with black eyes, white with red eyes, gold with red eyes (rare), and diluted grey with red eyes (rare). Two age points are shown here. The agouti mouse pictures are the same as used in Fig. 2 and Fig. 3. **(C, D)** The editing profiles and photos of mice not shown in Fig. 2 from Cas9 KO Experiment A and B. **(E**) Alignment of the two different types of 7-amino-acid deletions in MC1R (from mouse #533 and #536) with the wild-type MC1R protein sequence.

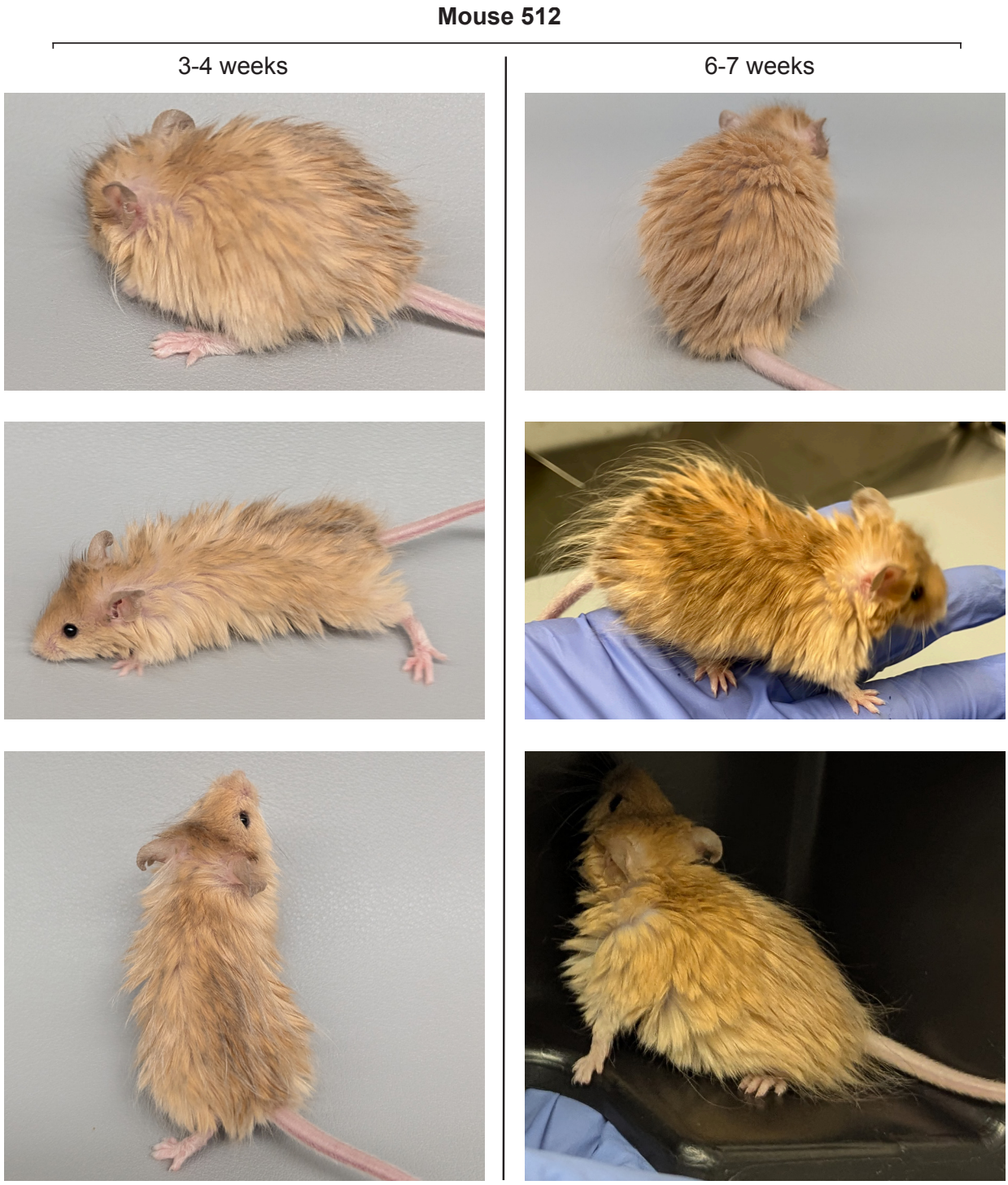

Fig. S2. Mouse #512 from Experiment A, at 3-4 weeks old and 6-7 weeks old.

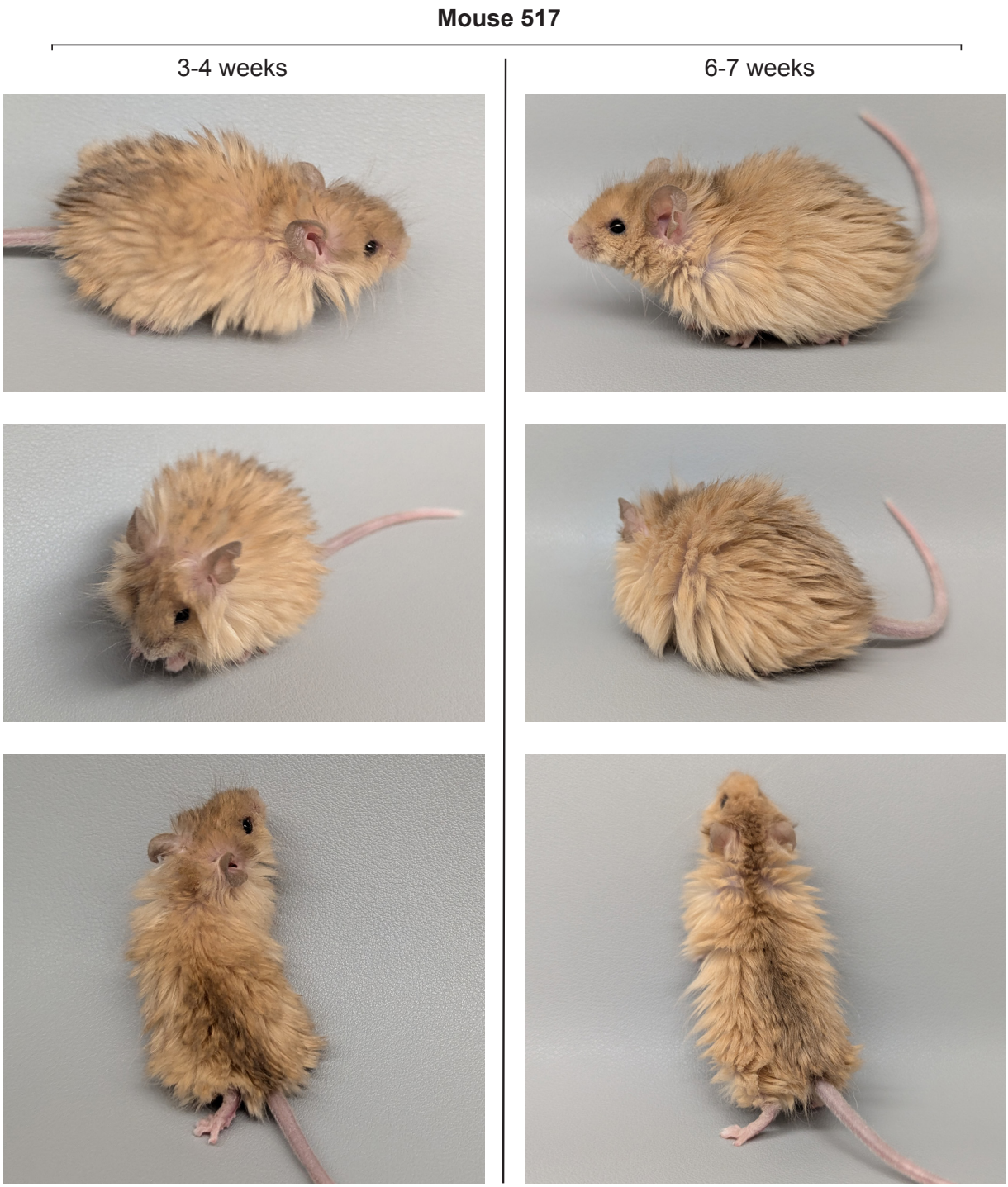

Fig. S3. Mouse #517 from Experiment A, at 3-4 weeks and 6-7 weeks old.

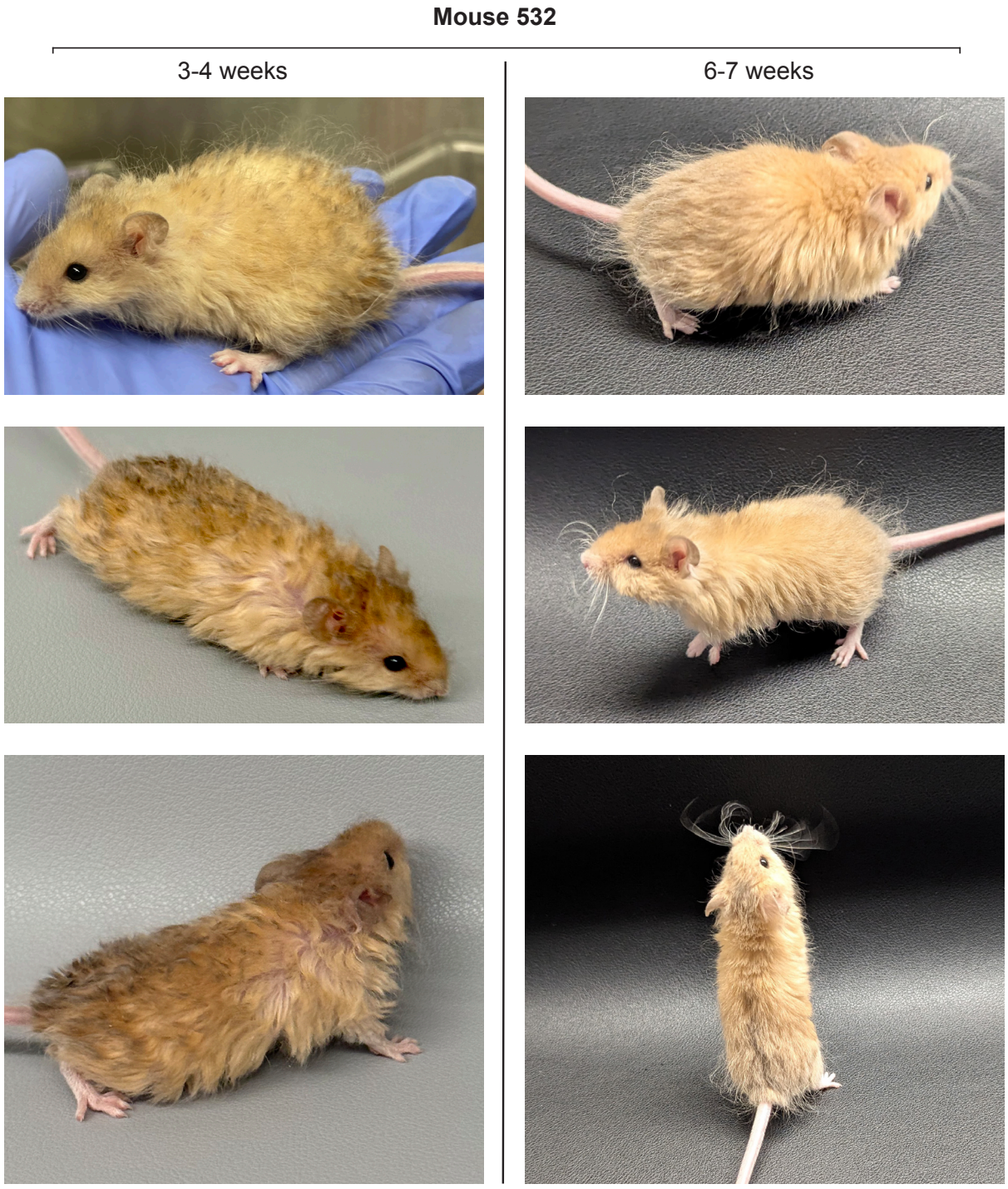

Fig. S4. Mouse #532 from Experiment B, at 3-4 weeks and 6-7 weeks old.

Fig. S5. Mouse #533 from Experiment B, at 3-4 weeks and 6-7 weeks old.

Fig. S6

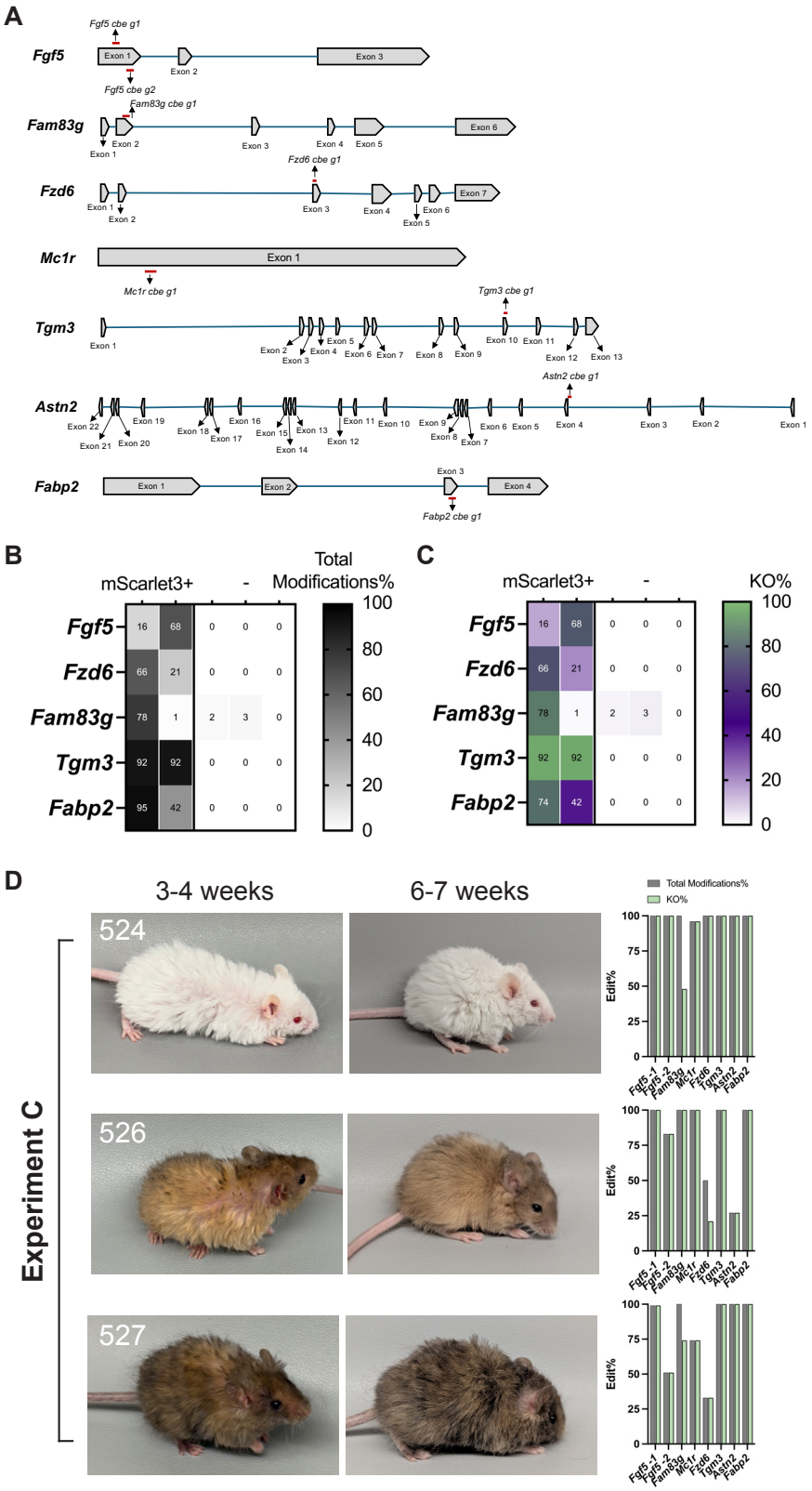
A
Fgf5
Fgf5 cbe g1
Fgf5 cbe g2
Fam83g
Fam83g cbe g1
Fzd6
Fzd6 cbe g1
Mc1r
Mc1r cbe g1
Tgm3
Tgm3 cbe g1
Astn2
Astn2 cbe g1
Fabp2
Fabp2 cbe g1
B
mScarlet3+
-
Total Modifications%
Fgf5
Fzd6
Fam83g
Tgm3
Fabp2
C
mScarlet3+
-
KO%
D
3-4 weeks
6-7 weeks
Experiment C
524
526
527
Total Modifications%
KO%
Edit%

Fig. S6. (A) Target genes and the location of their sgRNAs chosen for CBE KO animal production. We selected animal production sgRNA according to editing efficiency, off-target prediction, and the location of the C-to-T mutation. The ideal edit location should either mimic the previous literature or be in an early exon to facilitate KO. **(B, C)** Single embryo total modification% and KO% comparison between mScarlet3 + and mScarlet3 - embryos demonstrated in Fig. 3C. The individualized data represent the multiplexability and editing mosaicism in one animal by each condition. Each column is data from 1 embryo. Data was by Sanger sequencing. **(D)** The editing profiles and photos of mice not shown in Fig. 3 (Experiment C).

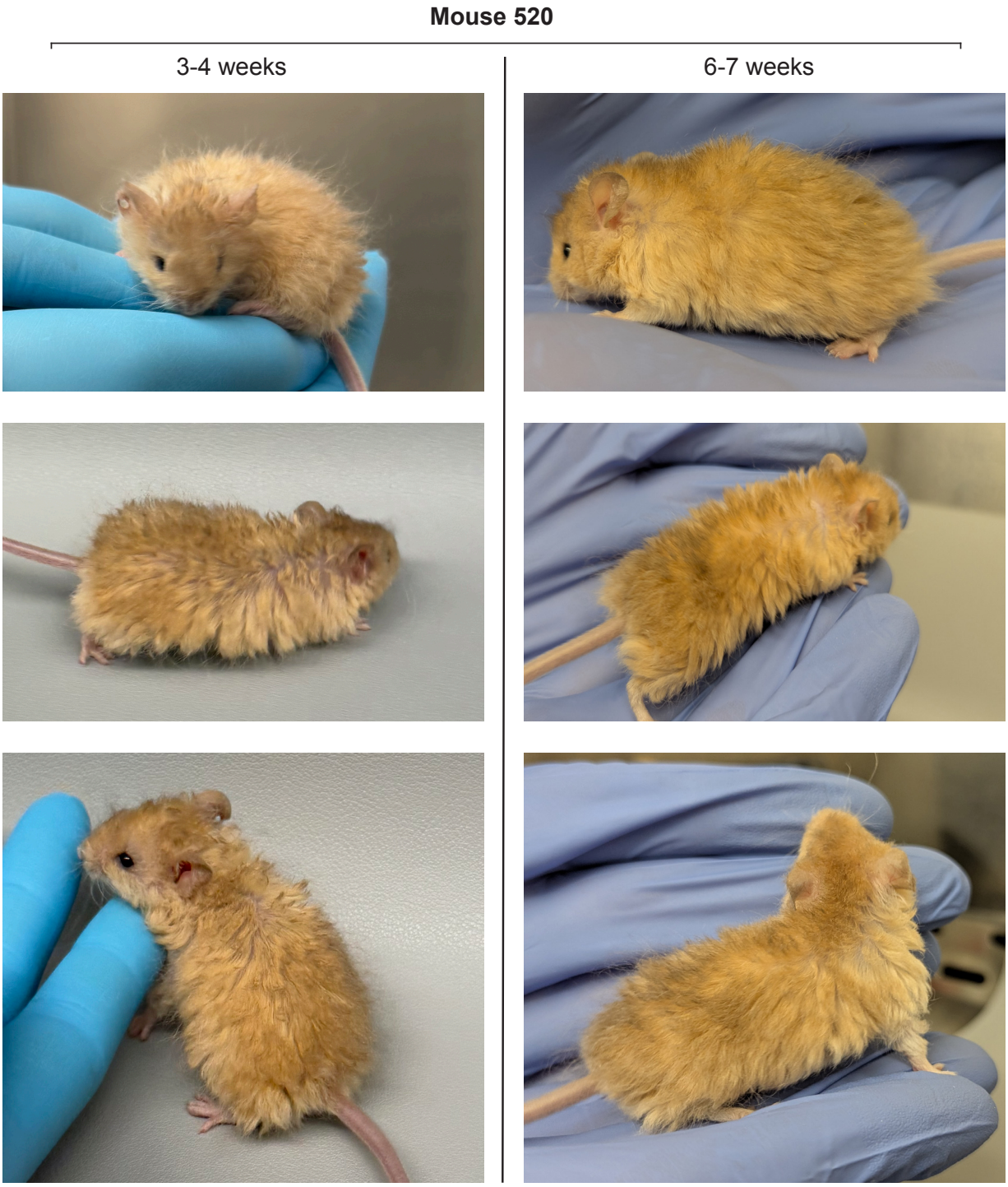

Fig. S7. Mouse #520 from Experiment C, at 3-4 weeks and 6-7 weeks old.

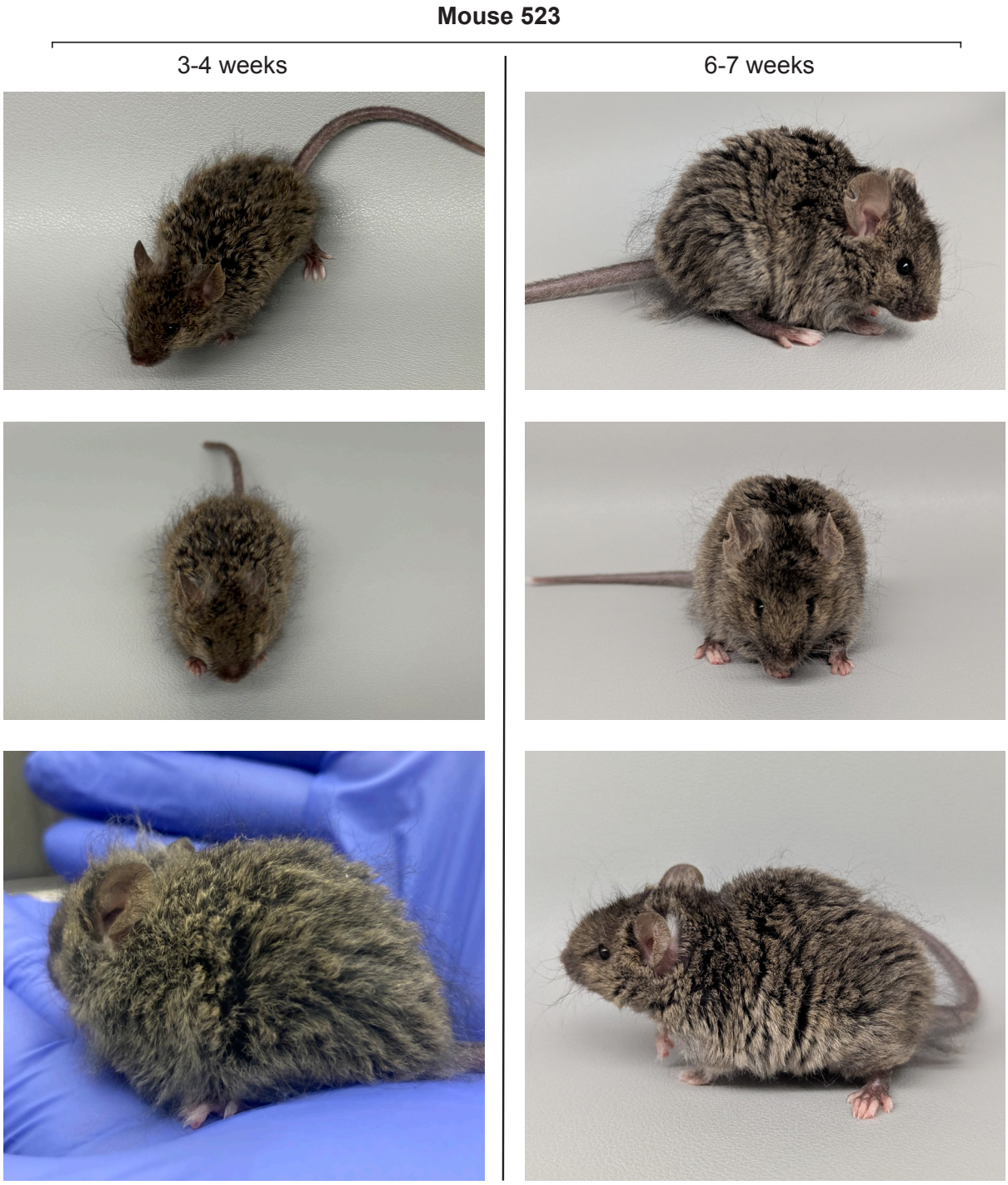

Fig. S8. Mouse #523 from Experiment C, at 3-4 weeks and 6-7 weeks old.

Fig. S9. Mouse #525 from Experiment C, at 3-4 weeks and 6-7 weeks old.

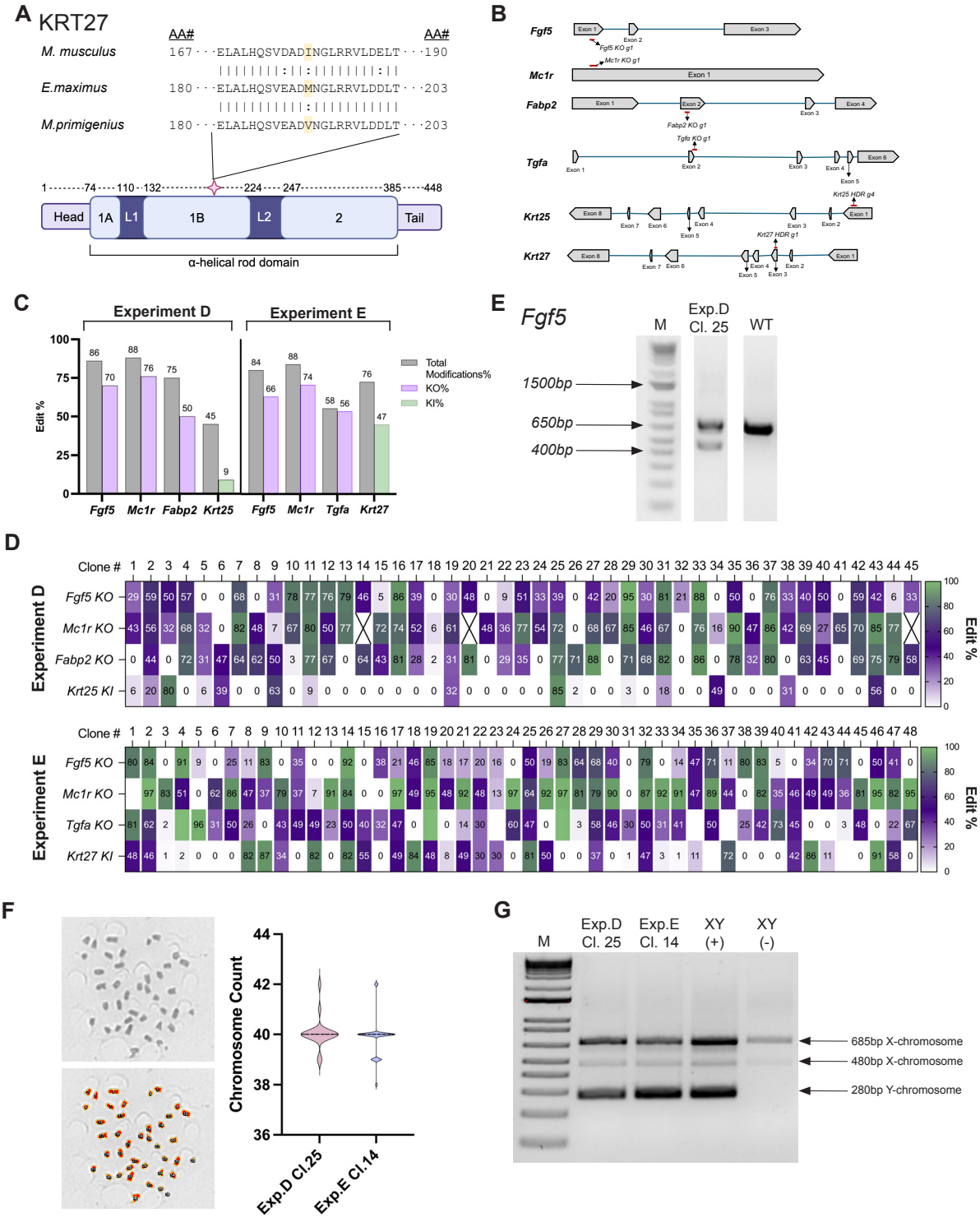

Fig. S10. (A) KRT27 protein alignment of *Mus musculus, Elephas maximus,* and *Mammuthus primigenius* centered around amino acid (AA) 191 (highlighted in yellow), a known fixed coding mutation between *E. maximus* (methionine) and *M. primigenius* (valine). In Experiment E, the *M. musculus* isoleucine was edited to *M. primigenius* valine via HDR. This mutation occurs in the

1B α-helical rod domain of the secondary structure of the KRT27 protein (star). **(B)** Target genes and the location of the sgRNAs selected for Cas9 KO and Cas9 HDR mESC generation. We selected production sgRNA for Cas9 KO and sgRNA/ssODN for Cas9 HDR according to editing efficiency, off-target prediction, and the location of the edit. **(C)** The KO% and KI% from Experiment D and E bulk mESC populations prior to single-cell sorting. **(D)** Preliminary KO and KI editing profiles for 45 clones generated in Experiment D and 48 clones generated in Experiment E. We collected clones from an iMEF feeder layer. **(E)** PCR analysis of *Fgf5* from Experiment D, clone 25, which shows a large deletion that was not initially identified by ICE analysis. DNA ladder is labeled as “M”. **(F)** Representative mESC metaphase spread used for chromosome counting. Images were acquired using an EVOS M7000 with 20X objective. Upper left is the original photo (greyscale); lower left is the same photo where chromosomes were recognized (highlighted by colors) and counted by ImageJ. We counted chromosomes from n = 20 (Experiment D) and n = 29 (Experiment E) edited mESCs. Experiment D, clone 25, was 80% normal with an average count of 40.05 chromosomes and median count of 40 chromosomes. Experiment E, clone 14, was 70% normal with an average count of 39.90 chromosomes and median count of 40 chromosomes. **(G)** XY PCR of Experiments D/E edited mESCs used for animal generation. The positive control (+) and negative control (-) are mESC lines characterized previously for internal use.

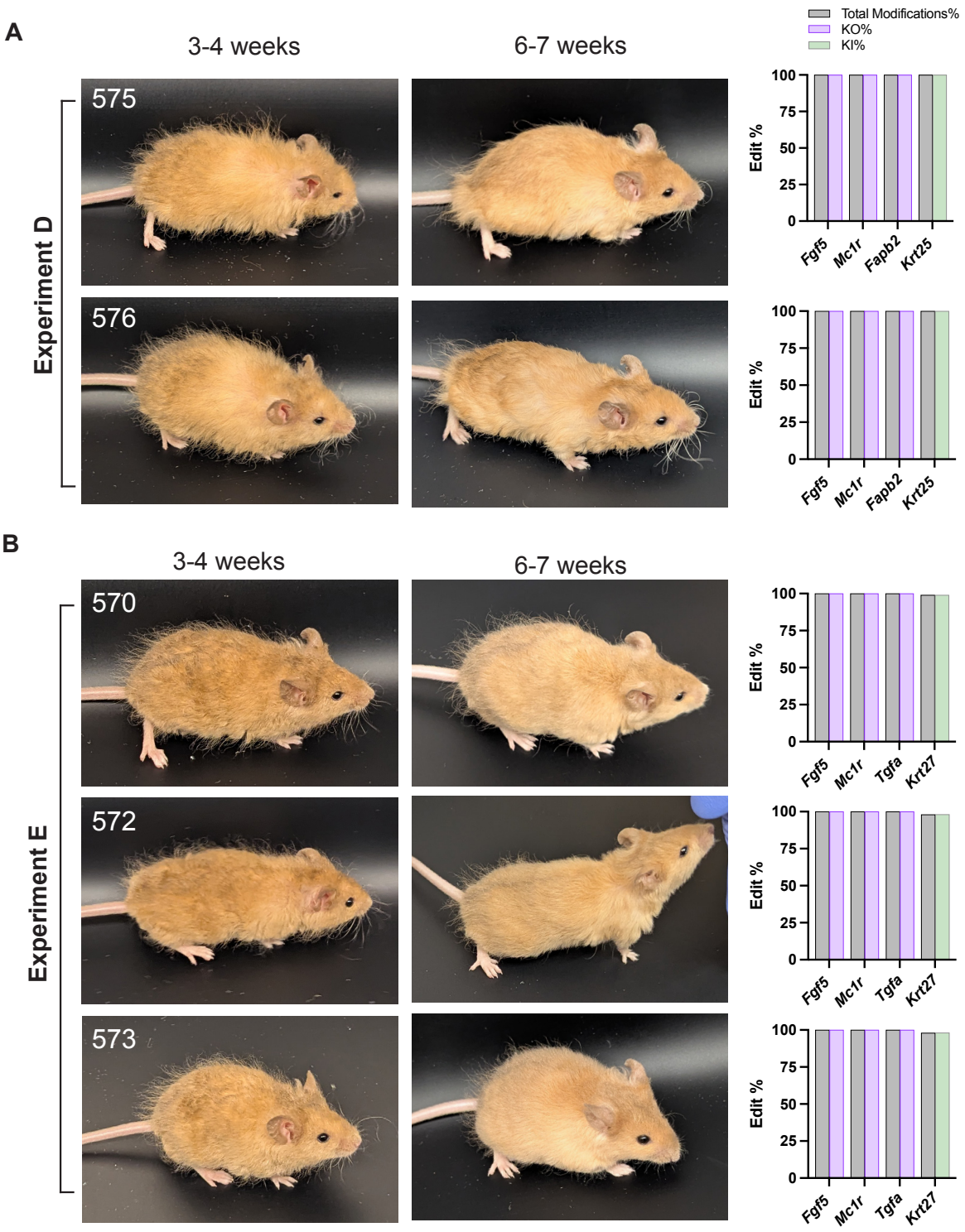

Fig. S11. (A) Editing profiles and photos of mice generated from Experiment D mESCs not shown in Fig. 5. **(B)** Editing profiles and photos of mice generated from Experiment E mESCs not shown in Fig. 5.

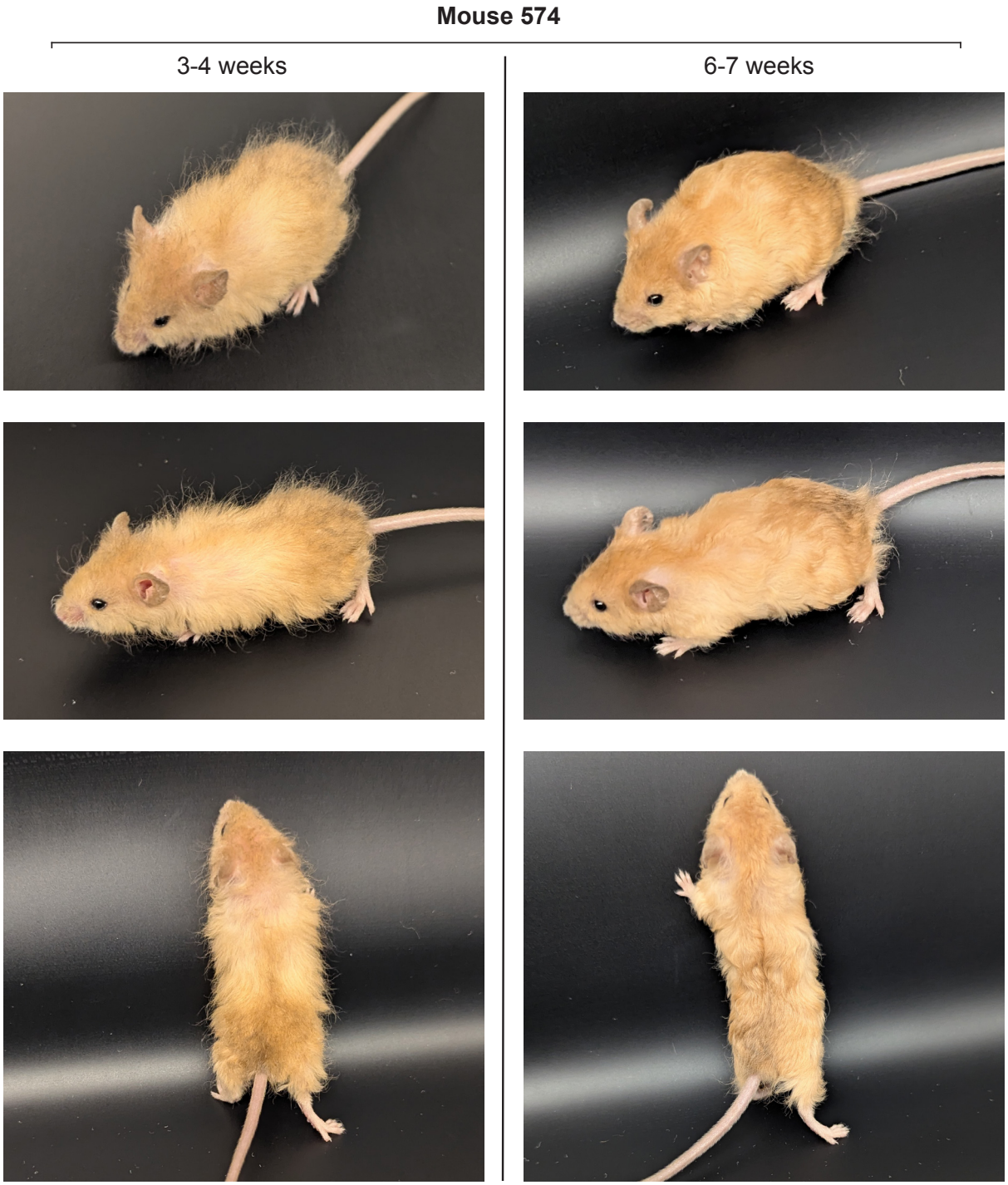

Fig. S12. Mouse #574 from Experiment D, at 3-4 weeks and 6-7 weeks old.

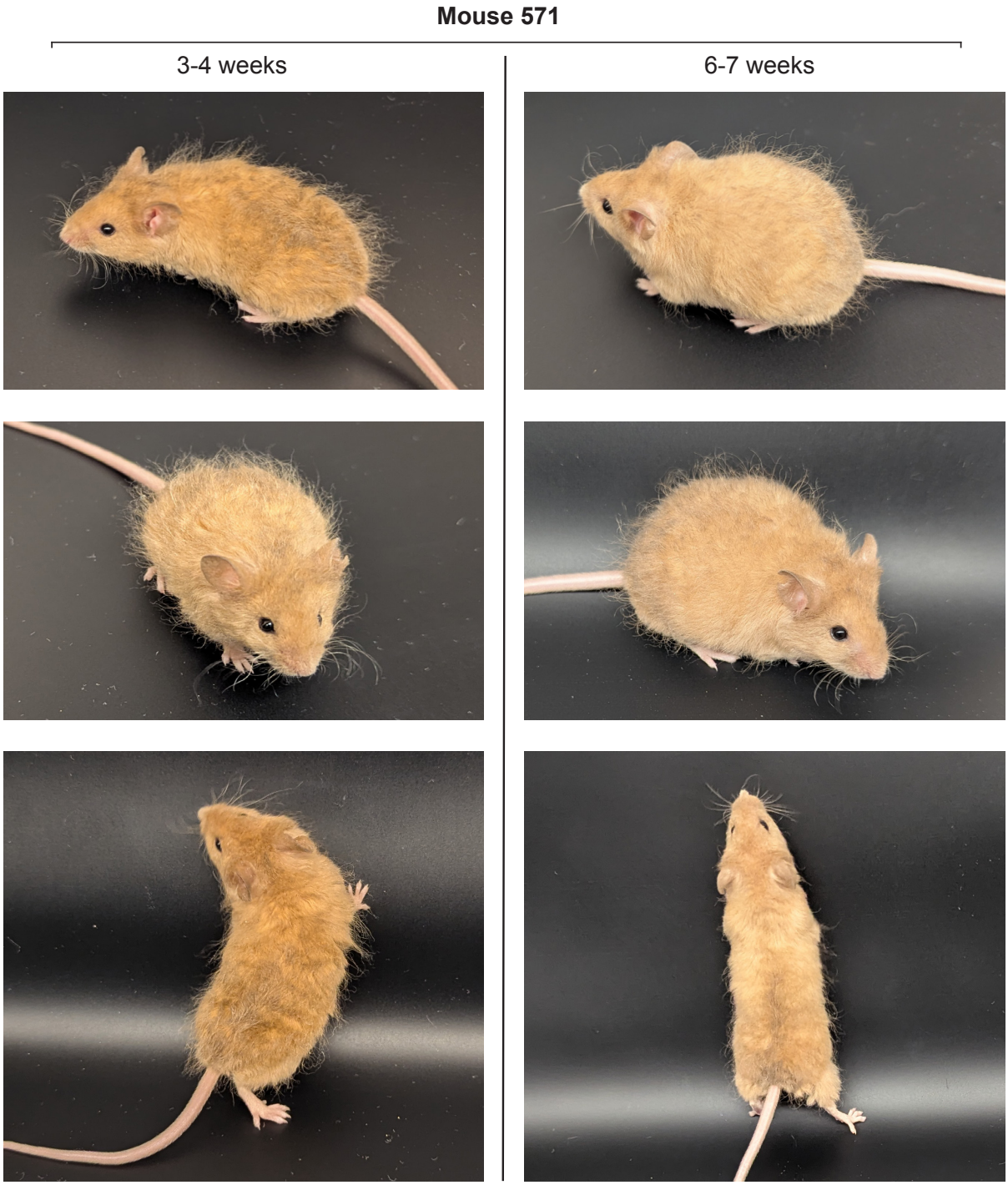

Fig. S13. Mouse #571 from Experiment E, at 3-4 weeks and 6-7 weeks old.

Supplement Tables

Table S1. High impact variants from mESC clone unbiased WGS off-target analysis

	Chr	Start	End	Gene	Ref	Alt	Annotation	VAF	Biotype
Exp.E-clone 14	chr11	107869130	107869130	*Prkca*	C	A	Missense variant	0.72	Protein coding

Table S2. mESC clone unbiased WGS off-target analysis summary

Clone	Impact	Variant Annotation	nVariants
Exp.D-clone 25	MODIFIER	intergenic_region	41
	MODIFIER	intron_variant	22
	MODIFIER	upstream_gene_variant	8
	MODIFIER	downstream_gene_variant	6
Exp.E-clone 14	MODERATE	missense_variant	1
	MODIFIER	intergenic_region	54
	MODIFIER	intron_variant	46
	MODIFIER	upstream_gene_variant	15
	MODIFIER	downstream_gene_variant	17
	MODIFIER	non_coding_transcript_exon_variant	2

Table S3. guide RNA and donor sequences used for mouse production experiment

Guide RNA

Exp No.	Gene	Colossal Guide ID	Spacer	Name used in this study	Other names used in this study
A	*Fam83g*	MMG83	TCTCCCAACACAGAATCTCA	*Fam83g g1*	
A	*Fgf5*	MMG189	TTTCCATCTGCAGATCTACC	*Fgf5 g1*	
A	*Fgf5*	MMG67	AGGAACCCGGGAGACTCCAG	*Fgf5 g2*	
A	*Fabp2*	MMG145	TCTGAAACTGACAATCACAC	*Fabp2 g1*	
A	*Fzd6*	MMG95	TTCATGTAGTTCTACCCTGT	*Fzd6 g1*	
A	*Mc1r*	MMG113	AGAGCACGACGGGCTGTCGT	*Mc1r g1*	*Mc1r cbe-g5*
B	*Fgf5*	MMG189	TTTCCATCTGCAGATCTACC	*Fgf5 g1*	
B	*Fgf5*	MMG67	AGGAACCCGGGAGACTCCAG	*Fgf5 g2*	
B	*Fabp2*	MMG145	TCTGAAACTGACAATCACAC	*Fabp2 g1*	
B	*Fam83g*	MMG83	TCTCCCAACACAGAATCTCA	*Fam83g g1*	
B	*Mc1r*	MMG157	GGTAAGTGTCAGCATCGTGC	*Mc1r g2*	
B	*Tgm3*	MMG166	GCCTGGACCATCGTCTACAA	*Tgm3 g1*	
C	*Fam83g*	MMG100	TGCCTACCGAGGTGTGACCC	*Fam83g cbe-g1*	
C	*Fgf5*	MMG11	AAGGGCAACCCGCGCCTCCT	*Fgf5 cbe-g1*	
C	*Tgm3*	MMG116	GTGCACCAAAAGGCTTTGGA	*Tgm3 cbe-g1*	
C	*Fgf5*	MMG12	TCTGCAGATCTACCCGGATG	*Fgf5 cbe-g2*	
C	*Fabp2*	MMG137	CTGTCCGAGAGGTTTCTGGT	*Fabp2 cbe-g1*	
C	*Mc1r*	MMG160	TCCACTCAGGAGCCCCAGAA	*Mc1r cbe-g1*	
C	*Fzd6*	MMG162	GCATCCGATGGCCTGAAGAA	*Fzd6 cbe-g1*	
C	*Astn2*	MMG177	TTCCCCCTGCAGAGAAGCAC	*Astn2 cbe-g1*	
D	*Fgf5*	MMG67	AGGAACCCGGGAGACTCCAG	*Fgf5 g1*	
D	*Mc1r*	MMG178	ATGGACACATACAGGCACCA	*Mc1r g1*	

D	*Krt25*	MMG142	CGCTTGCACGTTGTCCAGGT	*Krt25 g1*	
D	*Fabp2*	MMG145	TCTGAAACTGACAATCACAC	*Fabp2 g1*	
E	*Fgf5*	MMG67	AGGAACCCGGGAGACTCCAG	*Fgf5 g1*	
E	*Mc1r*	MMG178	ATGGACACATACAGGCACCA	*Mc1r g1*	
E	*Krt27*	MMG89	AGCGTCGATGCTGACATCAA	*Krt27 g1*	
E	*Tgfα*	MMG186	GATGGACTCACCACTCAGGG	*Tgfα g1*	

HDR donors

Exp No.	**Gene**	**Colossal Donor ID**	**Sequence**	**Name used in the related figures**
D	*Krt25*	DNR151	TGGCCTCCTGCAGCGCTTGCACGTTGTCCAGGTATGAGGCCTGGCGGTCATTAAGGTTCT	*d1*
E	*Krt27*	DNR142	GGCACTCCACCAGAGCGTCGATGCTGACgTCAATGGCTTGCGGAGGGTCCTGGATGAGCT	*d1*

Table S4. guide RNA and donor sequence used in screening and testing experiments by figures

Guide RNA

Figure	Gene	Colossal Guide ID	Spacer	Name used in the related figures
Fig2B	*Fabp2*	MMG145	TCTGAAACTGACAATCACAC	*Fabp2 g1*
Fig2B	*Fam83g*	MMG83	TCTCCCAACACAGAATCTCA	*Fam83g g1*
Fig2B	*Fam83g*	MMG82	TCTCAGGGTACGCAGCAGCG	*Fam83g g2*
Fig2B	*Fam83g*	MMG84	CATGCACCTGGGGCACCTCA	*Fam83g g3*
Fig2B	*Fam83g*	MMG85	GAGCGGGCCCGCATGCACCT	*Fam83g g4*
Fig2B	*Fgf5*	MMG189	TTTCCATCTGCAGATCTACC	*Fgf5 g1*
Fig2B	*Fgf5*	MMG67	AGGAACCCGGGAGACTCCAG	*Fgf5 g2*
Fig2B	*Fgf5*	MMG138	CAGGGGATTGTAGGAATACG	*Fgf5 g3*
Fig2B	*Fgf5*	MMG139	AAATATTTGCTGTGTCTCAG	*Fgf5 g4*
Fig2B	*Fzd6*	MMG95	TTCATGTAGTTCTACCCTGT	*Fzd6 g1*
Fig2B	*Fzd6*	MMG96	TTGGTATAAAAGCTTGGCAA	*Fzd6 g2*
Fig2B	*Mc1r*	MMG113	AGAGCACGACGGGCTGTCGT	*Mc1r g1*
Fig2B	*Mc1r*	MMG157	GGTAAGTGTCAGCATCGTGC	*Mc1r g2*
Fig2B	*Mc1r*	MMG155	TGGCTAGAAAGAAAGTGACG	*Mc1r g3*
Fig2B	*Mc1r*	MMG156	CACAGATGAGCACGTCAATG	*Mc1r g4*
Fig2B	*Mc1r*	MMG158	CCGCCAAGGCTTCTGCCTCA	*Mc1r g5*
Fig2B	*Mc1r*	MMG159	CGCCAAGGCTTCTGCCTCAA	*Mc1r g6*
Fig2B	*Mc1r*	MMG79	CCACCAACCAGTCAGAGCCT	*Mc1r g7*
Fig2B	*Mc1r*	MMG80	CTGTATGTGTCCATCCCAGA	*Mc1r g8*
Fig2B	*Tgm3*	MMG166	GCCTGGACCATCGTCTACAA	*Tgm3 g1*
Fig2B	*Tgm3*	MMG165	GTACCCTTGTCCACGAAGTG	*Tgm3 g2*
Fig2B	*Tgm3*	MMG164	GCTTGGTGCCACTCCGAGTG	*Tgm3 g3*
Fig2B	*Tgm3*	MMG122	AAGGGTACCATTGTAGACGA	*Tgm3 g4*
Fig2B	*Tgm3*	MMG121	TGACGATGAACATGACAGCC	*Tgm3 g5*
Fig2B	*Tgm3*	MMG119	GATTTGAGATTTTCCCCACT	*Tgm3 g6*
Fig2CDEF, Sup1CD	*Fgf5*	MMG139	AAATATTTGCTGTGTCTCAG	*Fgf5*
Fig2CDEF, Sup1CD	*Fabp2*	MMG145	TCTGAAACTGACAATCACAC	*Fabp2*
Fig2CD, Sup1C	*Fzd6*	MMG95	TTCATGTAGTTCTACCCTGT	*Fzd6*

Fig2CDEF, Sup1CD	*Fam83g*	MMG82	TCTCAGGGTACGCAGCAGCG	*Fam83g*
Fig2EF, Sup1D	*Tgm3*	MMG121	TGACGATGAACATGACAGCC	*Tgm3*
Fig2CDEF, Sup1CD	*Mc1r*	MMG113	AGAGCACGACGGGCTGTCGT	*Mc1r*
Fig3B	*Astn2*	MMG177	TTCCCCCTGCAGAGAAGCAC	*Astn2 cbe-g1*
Fig3B	*Astn2*	MMG175	CCCCCTGCAGAGAAGCACCA	*Astn2 cbe-g2*
Fig3B	*Astn2*	MMG176	TCCCCCTGCAGAGAAGCACC	*Astn2 cbe-g3*
Fig3B	*Fabp2*	MMG137	CTGTCCGAGAGGTTTCTGGT	*Fabp2 cbe-g1*
Fig3B	*Fam83g*	MMG100	TGCCTACCGAGGTGTGACCC	*Fam83g cbe-g1*
Fig3B	*Fam83g*	MMG99	CCTACCGAGGTGTGACCCGG	*Fam83g cbe-g2*
Fig3B	*Fam83g*	MMG102	CTTCACACGATCAGCCACCA	*Fam83g cbe-g3*
Fig3B	*Fam83g*	MMG101	ACACGATCAGCCACCAAGTT	*Fam83g cbe-g4*
Fig3B	*Fam83g*	MMG131	TCACACGATCAGCCACCAAG	*Fam83g cbe-g5*
Fig3B	*Fgf5*	MMG11	AAGGGCAACCCGCGCCTCCT	*Fgf5 cbe-g1*
Fig3B	*Fgf5*	MMG12	TCTGCAGATCTACCCGGATG	*Fgf5 cbe-g2*
Fig3B	*Fgf5*	MMG140	GATTCCAAGAAAACAGCTAT	*Fgf5 cbe-g3*
Fig3B	*Fgf5*	MMG136	GAATACGAGGAGTTTTCAGC	*Fgf5 cbe-g4*
Fig3B	*Fzd6*	MMG162	GCATCCGATGGCCTGAAGAA	*Fzd6 cbe-g1*
Fig3B	*Fzd6*	MMG153	CATCCGATGGCCTGAAGAAC	*Fzd6 cbe-g2*
Fig3B	*Fzd6*	MMG152	TTGCCAAGCTTTTATACCAA	*Fzd6 cbe-g3*
Fig3B	*Fzd6*	MMG154	CAGAGCAAATTCATGTAGTT	*Fzd6 cbe-g4*
Fig3B	*Fzd6*	MMG151	ATCCGATGGCCTGAAGAACT	*Fzd6 cbe-g5*
Fig3B	*Fzd6*	MMG132	TTTGCCAAGCTTTTATACCA	*Fzd6 cbe-g6*
Fig3B	*Fzd6*	MMG103	AGAGCAAATTCATGTAGTTC	*Fzd6 cbe-g7*
Fig3B	*Fzd6*	MMG105	CAGATCAAGTCCCAAGAGAC	*Fzd6 cbe-g8*
Fig3B	*Fzd6*	MMG104	CTTTGCCAAGCTTTTATACC	*Fzd6 cbe-g9*
Fig3B	*Fzd6*	MMG106	TCAGATCAAGTCCCAAGAGA	*Fzd6 cbe-g10*
Fig3B	*Fzd6*	MMG135	TGACCAGGGGATCGCTGCTG	*Fzd6 cbe-g11*
Fig3B	*Mc1r*	MMG160	TCCACTCAGGAGCCCCAGAA	*Mc1r cbe-g1*
Fig3B	*Mc1r*	MMG158	CCGCCAAGGCTTCTGCCTCA	*Mc1r cbe-g2*
Fig3B	*Mc1r*	MMG161	CCACTCAGGAGCCCCAGAAG	*Mc1r cbe-g3*
Fig3B	*Mc1r*	MMG159	CGCCAAGGCTTCTGCCTCAA	*Mc1r cbe-g4*

Fig3B	*Mc1r*	MMG113	AGAGCACGACGGGCTGTCGT	*Mc1r cbe-g5*
Fig3B	*Mc1r*	MMG111	GTGCAGCAGCTGGACAACCT	*Mc1r cbe-g6*
Fig3B	*Mc1r*	MMG112	GAGCACGACGGGCTGTCGTG	*Mc1r cbe-g7*
Fig3B	*Tgm3*	MMG116	GTGCACCAAAAGGCTTTGGA	*Tgm3 cbe-g1*
Fig3B	*Tgm3*	MMG115	GCACCAAAAGGCTTTGGACA	*Tgm3 cbe-g2*
Fig3B	*Tgm3*	MMG163	CATCCGATTTGAGATTTTCC	*Tgm3 cbe-g3*
Fig3B	*Tgm3*	MMG114	ATCCGATTTGAGATTTTCCC	*Tgm3 cbe-g4*
Fig3B	*Tgm3*	MMG118	GACCTACCTTGCAACCACGG	*Tgm3 cbe-g5*
Fig3B	*Tgm3*	MMG134	GGAAAGACAAGTGCACCAAA	*Tgm3 cbe-g6*
Fig3B	*Tgm3*	MMG117	CCTACCTTGCAACCACGGGT	*Tgm3 cbe-g7*
Fig3B	*Tgm3*	MMG133	GCATCCGATTTGAGATTTTC	*Tgm3 cbe-g8*
Fig3D Sup6BCD	*Fabp2*	MMG137	CTGTCCGAGAGGTTTCTGGT	*Fabp2*
Fig3D Sup6BCD	*Tgm3*	MMG116	GTGCACCAAAAGGCTTTGGA	*Tgm3*
Fig3D Sup6BCD	*Trpv3*	MMG110	TTTGTCCAAGCTGTACTTGT	*Trpv3*
Fig3D Sup6BCD	*Fgf5*	MMG12	TCTGCAGATCTACCCGGATG	*Fgf5*
Fig3D Sup6BCD	*Fzd6*	MMG132	TTTGCCAAGCTTTTATACCA	*Fzd6*
Fig3D Sup6BCD	*Fam83g*	MMG100	TGCCTACCGAGGTGTGACCC	*Fam83g*
Fig4B	*Tgfa*	MMG186	GATGGACTCACCACTCAGGG	*Tgfa g1*
Fig4B	*Tgfa*	MMG187	AACAGCACATCCCCCCTGAG	*Tgfa g2*
Fig4B	*Tgfa*	MMG188	TATCCTGTTAGCTGTGTGCC	*Tgfa g3*
Fig4B	*Tgfa*	MMG185	CAGAGCGAGCTGTCCGGTCG	*Tgfa g4*
Fig4B	*Fgf5*	MMG67	AGGAACCCGGGAGACTCCAG	*Fgf5 g1*
Fig4B	*Fgf5*	MMG139	AAATATTTGCTGTGTCTCAG	*Fgf5 g2*
Fig4B	*Fgf5*	MMG138	CAGGGGATTGTAGGAATACG	*Fgf5 g3*
Fig4B	*Mc1r*	MMG178	ATGGACACATACAGGCACCA	*Mc1r g1*
Fig4B	*Mc1r*	MMG157	GGTAAGTGTCAGCATCGTGC	*Mc1r g2*
Fig4B	*Mc1r*	MMG155	TGGCTAGAAAGAAAGTGACG	*Mc1r g3*
Fig4B	*Mc1r*	MMG113	AGAGCACGACGGGCTGTCGT	*Mc1r g4*
Fig4B	*Mc1r*	MMG80	CTGTATGTGTCCATCCCAGA	*Mc1r g5*
Fig4B	*Mc1r*	MMG156	CACAGATGAGCACGTCAATG	*Mc1r g6*

Fig4B	*Mc1r*	MMG79	CCACCAACCAGTCAGAGCCT	*Mc1r g7*
Fig4B	*Krt25*	MMG142	CGCTTGCACGTTGTCCAGGT	*Krt25 g1*
Fig4B	*Krt25*	MMG143	TTGCACGTTGTCCAGGTAGG	*Krt25 g2*
Fig4B	*Krt27*	MMG89	AGCGTCGATGCTGACATCAA	*Krt27 g1*
Fig4B	*Krt27*	MMG88	ATGCTGACATCAATGGCTTG	*Krt27 g2*

HDR donors

Figure	**Gene**	**Colossal Donor ID**	**Sequence**	**Name used in the related figures**
Fig4B	*Krt25*	DNR151	TGGCCTCCTGCAGCGCTTGCA CGTTGTCCAGGTATGAGGCCT GGCGGTCATTAAGGTTCT	*d1*
Fig4B	*Krt25*	DNR160	CCTTGATCTTCTGCTCCAGGT CAGCGTTGGCCTCCTGCAGC GCTTGCACGTTGTCCAGGTAG GAGGCCtGGCGGTCATTAAGG TTCTGCATGGTCACCTTCTCAT TGCCGGAGAGGAGCC	*d2*
Fig4B	*Krt27*	DNR142	GGCACTCCACCAGAGCGTCG ATGCTGACgTCAATGGCTTGC GGAGGGTCCTGGATGAGCT	*d1*
Fig4B	*Krt27*	DNR141	ACTGGCACTCCACCAGAGCGT CGATGCTGACgTCAATGGCTT GCGGAGGGTCCTGGATGAGC TGACCCTGTGCAGAACCG	*d2*

Table S5. Cas9, sgRNA, donor concentration for CRISPR/Cas9 RNP electroporation

Experiment	Gene targets[1]	No. of sgRNA	Cas9 Nuclease concentration (μM)	sgRNA concentration (each, μM)	Electroporation enhancer (μM)
A	***Fgf5***, *Fabp2*, *Mc1r*, *Fzd6*, *Fam83g*	6	6	1	4
B	***Fgf5***, *Fabp2*, *Mc1r*, *Fzd6*, *Trpv3*	6	6	1	4

[1]Bold gene targets indicate that two sgRNAs were used.

Table S6. CBE mRNA and sgRNA concentration for CBE pronuclear injection

Experiment	Gene targets[1]	sgRNA concentration (each, ng/μL)	No. of sgRNA	CBE concentration (ng/μL)
C	***Fgf5***, *Fabp2*, *Mc1r*, *Fam83g*, *Fzd6*, *Tgm3*, *Astn2*	25	8	200

[1]Bold gene targets indicate that two sgRNAs were used.

Table S7. Genotyping primers for NGS and Sanger sequencing.

Lower cases are NGS adaptor sequences.

Gene	Colossal Guide ID	Sanger Forward Primer	Sanger Reverse Primer	NGS Forward Primer	NGS Reverse Primer
Astn2	MMG175	AATACGCAGGGCAGTTCTGG	ATCAGGAGAAGCCCAGGGAT	tcgtcggcagcgtcagatgtgtataagagacagAATACGCAGGGCAGTTCTGG	gtctcgtgggctcggagatgtgtataagagacagATCAGGAGAAGCCCAGGGAT
Astn2	MMG176	AATACGCAGGGCAGTTCTGG	ATCAGGAGAAGCCCAGGGAT	tcgtcggcagcgtcagatgtgtataagagacagAATACGCAGGGCAGTTCTGG	gtctcgtgggctcggagatgtgtataagagacagATCAGGAGAAGCCCAGGGAT
Astn2	MMG177	AATACGCAGGGCAGTTCTGG	ATCAGGAGAAGCCCAGGGAT	tcgtcggcagcgtcagatgtgtataagagacagAATACGCAGGGCAGTTCTGG	gtctcgtgggctcggagatgtgtataagagacagATCAGGAGAAGCCCAGGGAT
Fabp2	MMG137	TTCCTATCATCCAGAGGGTCACT	ATCGCTTGGCCTCAACTCCT	tcgtcggcagcgtcagatgtgtataagagacagTCCAGAGGGTCACTGTGAGT	gtctcgtgggctcggagatgtgtataagagacagACTCAAAATCACCTTGTCTTTGGA
Fabp2	MMG145	AGCAAGGCAAAACAGAACTTGG	CCGTTCCGTCTGCTAGACTG	tcgtcggcagcgtcagatgtgtataagagacagAGCAAGGCAAAACAGAACTTGG	gtctcgtgggctcggagatgtgtataagagacagCCGTTCCGTCTGCTAGACTG
Fam83g	MMG100	GTATCGTGGAGGCCATCGAG	CTCCTGGGTCTGAGACGAGA	tcgtcggcagcgtcagatgtgtataagagacagGAACCCCAGGACAACGGAG	gtctcgtgggctcggagatgtgtataagagacagGTGAATGGGGGTCTCGCC
Fam83g	MMG101	TTCTCCACCTTGCACCTCAC	CCCAAGCTGCAGAGGAGAAT	tcgtcggcagcgtcagatgtgtataagagacagTTCTCCACCTTGCACCTCAC	gtctcgtgggctcggagatgtgtataagagacagCCCAAGCTGCAGAGGAGAAT
Fam83g	MMG102	TTCTCCACCTTGCACCTCAC	CCCAAGCTGCAGAGGAGAAT	tcgtcggcagcgtcagatgtgtataagagacagTTCTCCACCTTGCACCTCAC	gtctcgtgggctcggagatgtgtataagagacagCCCAAGCTGCAGAGGAGAAT

Fam83g	MMG131	TTCTCCACCTTGCACCTCAC	CCCAAGCTGCAGAGGAGAAT	tcgtcggcagcgtcagatgtgtataagagacagTTCTCCACCTTGCACCTCAC	gtctcgtgggctcggagatgtgtataagagacagCCCAAGCTGCAGAGGAGAAT
Fam83g	MMG82	TTCTCCACCTTGCACCTCAC	CCCAAGCTGCAGAGGAGAAT	tcgtcggcagcgtcagatgtgtataagagacagTTCTCCACCTTGCACCTCAC	gtctcgtgggctcggagatgtgtataagagacagCCCAAGCTGCAGAGGAGAAT
Fam83g	MMG83	TTCTCCACCTTGCACCTCAC	CCCAAGCTGCAGAGGAGAAT	tcgtcggcagcgtcagatgtgtataagagacagTTCTCCACCTTGCACCTCAC	gtctcgtgggctcggagatgtgtataagagacagCCCAAGCTGCAGAGGAGAAT
Fam83g	MMG84	CCCAGTCTTTTCCTGTTCCCA	TTGGTATAAGGCACTGTCTGC	tcgtcggcagcgtcagatgtgtataagagacagCCCAGTCTTTTCCTGTTCCCA	gtctcgtgggctcggagatgtgtataagagacagTTGGTATAAGGCACTGTCTGC
Fam83g	MMG85	CCCAGTCTTTTCCTGTTCCCA	TTGGTATAAGGCACTGTCTGC	tcgtcggcagcgtcagatgtgtataagagacagCCCAGTCTTTTCCTGTTCCCA	gtctcgtgggctcggagatgtgtataagagacagTTGGTATAAGGCACTGTCTGC
Fam83g	MMG99	GTATCGTGGAGGCCATCGAG	CTCCTGGGTCTGAGACGAGA	tcgtcggcagcgtcagatgtgtataagagacagGAACCCCAGGACAACGGAG	gtctcgtgggctcggagatgtgtataagagacagGTGAATGGGGGTCTCGCC
Fgf5	MMG11	GAGGCTATGTCCACCCTGTG	CACGAAACCCTACCGGACTC	tcgtcggcagcgtcagatgtgtataagagacagAAGATGCACTTAGGACCCCC	gtctcgtgggctcggagatgtgtataagagacagAAGGGCTCCACTGGAAACTG
Fgf5	MMG12	GAGGCTATGTCCACCCTGTG	CACGAAACCCTACCGGACTC	tcgtcggcagcgtcagatgtgtataagagacagGTAGCGCGACGTTTTCTTCG	gtctcgtgggctcggagatgtgtataagagacagGTCCCTCCCAGAACAGGTTT
Fgf5	MMG136	TCCGAGTGTACACGCATTGT	ACCGGTGGAGCACTTTTCAA	tcgtcggcagcgtcagatgtgtataagagacagGACATTGAATTCTTCACAGTTCTGTG	gtctcgtgggctcggagatgtgtataagagacagAACAATCTCTTCACTTTGTTACAGACG

Fgf5	MMG138	TCCGAGTGTACACGCATTGT	ACCGGTGGAGCACTTTTCAA	tcgtcggcagcgtcagatgtgtataagagacagGACATTGAATTCTTCACAGTTCTGTG	gtctcgtgggctcggagatgtgtataagagacagAACAATCTCTTCACTTTGTTACAGACG
Fgf5	MMG139	TCCGAGTGTACACGCATTGT	ACCGGTGGAGCACTTTTCAA	tcgtcggcagcgtcagatgtgtataagagacagGACATTGAATTCTTCACAGTTCTGTG	gtctcgtgggctcggagatgtgtataagagacagAACAATCTCTTCACTTTGTTACAGACG
Fgf5	MMG140	GGGAACAGAATAAGGGTATCCC	GTTTGACCCGTGGGCTGC	tcgtcggcagcgtcagatgtgtataagagacagGGGAACAGAATAAGGGTATCCC	gtctcgtgggctcggagatgtgtataagagacagGTTTGACCCGTGGGCTGC
Fgf5	MMG189	GAGGCTATGTCCACCCTGTG	CACGAAACCCTACCGGACTC	tcgtcggcagcgtcagatgtgtataagagacagTCTTCTGCCTCCTCACCAGT	gtctcgtgggctcggagatgtgtataagagacagAGCAGAGTCCCAGACGCTA
Fgf5	MMG67 300x NGS	GAGGCTATGTCCACCCTGTG	CACGAAACCCTACCGGACTC	tcgtcggcagcgtcagatgtgtataagagacagAAGATGCACTTAGGACCCCC	gtctcgtgggctcggagatgtgtataagagacagAAGGGCTCCACTGGAAACTG
Fgf5	MMG67, MMG189 500x NGS	GAGGCTATGTCCACCCTGTG	CACGAAACCCTACCGGACTC	tcgtcggcagcgtcagatgtgtataagagacagAAGATGCACTTAGGACCCCC	gtctcgtgggctcggagatgtgtataagagacagAGCAGAGTCCCAGACGCTA
Fzd6	MMG103	GACTCATTTCGAAGGTAGGTGA	TTCTTCAGGCCATCGGATGC	tcgtcggcagcgtcagatgtgtataagagacagGACTCATTTCGAAGGTAGGTGA	gtctcgtgggctcggagatgtgtataagagacagTTCTTCAGGCCATCGGATGC
Fzd6	MMG104	GACTCATTTCGAAGGTAGGTGA	TTCTTCAGGCCATCGGATGC	tcgtcggcagcgtcagatgtgtataagagacagGACTCATTTCGAAGGTAGGTGA	gtctcgtgggctcggagatgtgtataagagacagTTCTTCAGGCCATCGGATGC
Fzd6	MMG105	GGAGTGAAGGGAAGGGGGAA	AGGAACGTGAACAGAGTTGCA	tcgtcggcagcgtcagatgtgtataagagacagTGTAAACTTTACAGATTGCCACAC	gtctcgtgggctcggagatgtgtataagagacagTACATATTGGGGCACGGAGG

Fzd6	MMG106	GGAGTGAAGGGAAGGGGGAA	AGGAACGTGAACAGAGTTGCA	tcgtcggcagcgtcagatgtgtataagagacagTGTAAACTTTACAGATTGCCACAC	gtctcgtgggctcggagatgtgtataagagacagTACATATTGGGGCACGGAGG
Fzd6	MMG132	GACTCATTTCGAAGGTAGGTGA	TTCTTCAGGCCATCGGATGC	tcgtcggcagcgtcagatgtgtataagagacagGACTCATTTCGAAGGTAGGTGA	gtctcgtgggctcggagatgtgtataagagacagTTCTTCAGGCCATCGGATGC
Fzd6	MMG135	TGGCAAGATGGAAAGGTCCC	TTTCAATATAGGCATGAAAATCCACT	tcgtcggcagcgtcagatgtgtataagagacagTGGCAAGATGGAAAGGTCCC	gtctcgtgggctcggagatgtgtataagagacagTTTCAATATAGGCATGAAAATCCACT
Fzd6	MMG151	TGAAATGTTCCTTTGCCAAGCT	ACGCGCTAACAATACTAAAGTGC	tcgtcggcagcgtcagatgtgtataagagacagTGAAATGTTCCTTTGCCAAGCT	gtctcgtgggctcggagatgtgtataagagacagACGCGCTAACAATACTAAAGTGC
Fzd6	MMG152	GACTCATTTCGAAGGTAGGTGA	TTCTTCAGGCCATCGGATGC	tcgtcggcagcgtcagatgtgtataagagacagGACTCATTTCGAAGGTAGGTGA	gtctcgtgggctcggagatgtgtataagagacagTTCTTCAGGCCATCGGATGC
Fzd6	MMG153	TGAAATGTTCCTTTGCCAAGCT	ACGCGCTAACAATACTAAAGTGC	tcgtcggcagcgtcagatgtgtataagagacagTGAAATGTTCCTTTGCCAAGCT	gtctcgtgggctcggagatgtgtataagagacagACGCGCTAACAATACTAAAGTGC
Fzd6	MMG154	GACTCATTTCGAAGGTAGGTGA	TTCTTCAGGCCATCGGATGC	tcgtcggcagcgtcagatgtgtataagagacagGACTCATTTCGAAGGTAGGTGA	gtctcgtgggctcggagatgtgtataagagacagTTCTTCAGGCCATCGGATGC
Fzd6	MMG162	TGAAATGTTCCTTTGCCAAGCT	ACGCGCTAACAATACTAAAGTGC	tcgtcggcagcgtcagatgtgtataagagacagTGAAATGTTCCTTTGCCAAGCT	gtctcgtgggctcggagatgtgtataagagacagACGCGCTAACAATACTAAAGTGC

Fzd6	MMG95	GACTCATTTCGAAGGTAGGTGA	TTCTTCAGGCCATCGGATGC	tcgtcggcagcgtcagatgtgtataagagacagGACTCATTTCGAAGGTAGGTGA	gtctcgtgggctcggagatgtgtataagagacagTTCTTCAGGCCATCGGATGC
Fzd6	MMG96	GACTCATTTCGAAGGTAGGTGA	TTCTTCAGGCCATCGGATGC	tcgtcggcagcgtcagatgtgtataagagacagGACTCATTTCGAAGGTAGGTGA	gtctcgtgggctcggagatgtgtataagagacagTTCTTCAGGCCATCGGATGC
Krt25	MMG142	TCCAATGCCCTTAAATGCCC	TTCGCCTTTCCAGTGGATCC	tcgtcggcagcgtcagatgtgtataagagacagTAGTCATGATCGAGACCGCG	gtctcgtgggctcggagatgtgtataagagacagTGTGCTGGCTTCACTGTGAA
Krt27	MMG89	GGAAGGTTGGGTGCCTACC	TGGGGTGACTCAAATCTGGC	tcgtcggcagcgtcagatgtgtataagagacagGGAAGGTTGGGTGCCTACC	gtctcgtgggctcggagatgtgtataagagacagTGGGGTGACTCAAATCTGGC
Mc1r	MMG111	GAGACCCCCGACAACAACAT	AGAAAGTGACGAGGCAGAGC	tcgtcggcagcgtcagatgtgtataagagacagGCATCGTGCTGGAGACTACT	gtctcgtgggctcggagatgtgtataagagacagAAGAGGGTGCTGGAGACGAT
Mc1r	MMG112	GAGACCCCCGACAACAACAT	AGAAAGTGACGAGGCAGAGC	tcgtcggcagcgtcagatgtgtataagagacagGCATCGTGCTGGAGACTACT	gtctcgtgggctcggagatgtgtataagagacagAAGAGGGTGCTGGAGACGAT
Mc1r	MMG113	GAGACCCCCGACAACAACAT	AGAAAGTGACGAGGCAGAGC	tcgtcggcagcgtcagatgtgtataagagacagGCATCGTGCTGGAGACTACT	gtctcgtgggctcggagatgtgtataagagacagAAGAGGGTGCTGGAGACGAT
Mc1r	MMG155	TCCATCTTCTATGCGCTGCG	TTTTGTGGAGCTGGGCAATG	tcgtcggcagcgtcagatgtgtataagagacagTCCATCTTCTATGCGCTGCG	gtctcgtgggctcggagatgtgtataagagacagTTTTGTGGAGCTGGGCAATG
Mc1r	MMG156	GAGACCCCCGACAACAACAT	AGAAAGTGACGAGGCAGAGC	tcgtcggcagcgtcagatgtgtataagagacagGCATCGTGCTGGAGACTACT	gtctcgtgggctcggagatgtgtataagagacagAAGAGGGTGCTGGAGACGAT

Mc1r	MMG157	GAGACCCCC GACAACAACA T	AGAAAGTGAC GAGGCAGAG C	tcgtcggcagcgtc agatgtgtataaga gacagGGAGC CCCAGAAGA GTCTTC	gtctcgtgggctcgg agatgtgtataaga gacagCCTCCA GCAGCAGGA TGATAG
Mc1r	MMG158	CTGCTCTGCC TCGTCACTTT	GGCAGAGGA CGATGAGCAA G	tcgtcggcagcgtc agatgtgtataaga gacagCTGCTC TGCCTCGTCA CTTT	gtctcgtgggctcgg agatgtgtataaga gacagGGCAG AGGACGATG AGCAAG
Mc1r	MMG159	CTGCTCTGCC TCGTCACTTT	GGCAGAGGA CGATGAGCAA G	tcgtcggcagcgtc agatgtgtataaga gacagCTGCTC TGCCTCGTCA CTTT	gtctcgtgggctcgg agatgtgtataaga gacagGGCAG AGGACGATG AGCAAG
Mc1r	MMG160	AAAATCGGAG CGTGCCTGTA	AAGGCTCTGA CTGGTTGGTG	tcgtcggcagcgtc agatgtgtataaga gacagAAAATC GGAGCGTGC CTGTA	gtctcgtgggctcgg agatgtgtataaga gacagAAGGCT CTGACTGGTT GGTG
Mc1r	MMG161	AAAATCGGAG CGTGCCTGTA	AAGGCTCTGA CTGGTTGGTG	tcgtcggcagcgtc agatgtgtataaga gacagAAAATC GGAGCGTGC CTGTA	gtctcgtgggctcgg agatgtgtataaga gacagAAGGCT CTGACTGGTT GGTG
Mc1r	MMG178	CTCCACAGAC CGCTTCCTAC	ACCAGCACAT TCTCCACCAG	tcgtcggcagcgtc agatgtgtataaga gacagCTCCAC AGACCGCTTC CTAC	gtctcgtgggctcgg agatgtgtataaga gacagACCAGC ACATTCTCCA CCAG
Mc1r	MMG79	GAGACCCCC GACAACAACA T	AGAAAGTGAC GAGGCAGAG C	tcgtcggcagcgtc agatgtgtataaga gacagGGAGC CCCAGAAGA GTCTTC	gtctcgtgggctcgg agatgtgtataaga gacagCCTCCA GCAGCAGGA TGATAG
Mc1r	MMG80	GAGACCCCC GACAACAACA T	AGAAAGTGAC GAGGCAGAG C	tcgtcggcagcgtc agatgtgtataaga gacagGGAGC CCCAGAAGA GTCTTC	gtctcgtgggctcgg agatgtgtataaga gacagCCTCCA GCAGCAGGA TGATAG
Tgfa	MMG186	CATCGAGCC CCTCAAAGGA G	TCCCTGGGAA GGAGCTTTCT	tcgtcggcagcgtc agatgtgtataaga gacagCATCGA GCCCCTCAAA GGAG	gtctcgtgggctcgg agatgtgtataaga gacagTCCCTG GGAAGGAGC TTTCT

Tgm3	MMG114	AAGACTACCTGTCCCCTCCC	AGAAGTCCATGTCTGGCAGC	tcgtcggcagcgtcagatgtgtataagagacagCATGTAGCCTGAGCCCTCTG	gtctcgtgggctcggagatgtgtataagagacagGGGTCGGTCACTCAGAGACA
Tgm3	MMG115	TGGGAGCATTTTGGACAGGT	ATGCTGGGCTCCTTGTCTTC	tcgtcggcagcgtcagatgtgtataagagacagTGGGAGCATTTTGGACAGGT	gtctcgtgggctcggagatgtgtataagagacagATGCTGGGCTCCTTGTCTTC
Tgm3	MMG116	TGGGAGCATTTTGGACAGGT	ATGCTGGGCTCCTTGTCTTC	tcgtcggcagcgtcagatgtgtataagagacagTGGGAGCATTTTGGACAGGT	gtctcgtgggctcggagatgtgtataagagacagATGCTGGGCTCCTTGTCTTC
Tgm3	MMG117	CAACCCTCTGAGTCAGCCAG	CACAGCCAGGTAAGTGCAGA	tcgtcggcagcgtcagatgtgtataagagacagTCTGGCCATTGCTATTGCCA	gtctcgtgggctcggagatgtgtataagagacagCCACAGGCTTTCTCCAACCA
Tgm3	MMG118	CAACCCTCTGAGTCAGCCAG	CACAGCCAGGTAAGTGCAGA	tcgtcggcagcgtcagatgtgtataagagacagTCTGGCCATTGCTATTGCCA	gtctcgtgggctcggagatgtgtataagagacagCCACAGGCTTTCTCCAACCA
Tgm3	MMG119	AAGACTACCTGTCCCCTCCC	AGAAGTCCATGTCTGGCAGC	tcgtcggcagcgtcagatgtgtataagagacagCATGTAGCCTGAGCCCTCTG	gtctcgtgggctcggagatgtgtataagagacagGGGTCGGTCACTCAGAGACA
Tgm3	MMG121	ATGCACAGGTTCCAGTGAGG	AAGGCTTTACCCATGGAGGC	tcgtcggcagcgtcagatgtgtataagagacagGAAGGGGAAGACAAGGAGCC	gtctcgtgggctcggagatgtgtataagagacagGTGAGCAACTCTTTTGGGCC
Tgm3	MMG122	ATGCACAGGTTCCAGTGAGG	AAGGCTTTACCCATGGAGGC	tcgtcggcagcgtcagatgtgtataagagacagGAAGGGGAAGACAAGGAGCC	gtctcgtgggctcggagatgtgtataagagacagGTGAGCAACTCTTTTGGGCC
Tgm3	MMG133	AAGACTACCTGTCCCCTCCC	AGAAGTCCATGTCTGGCAGC	tcgtcggcagcgtcagatgtgtataagagacagCATGTAGCCTGAGCCCTCTG	gtctcgtgggctcggagatgtgtataagagacagGGGTCGGTCACTCAGAGACA

Tgm3	MMG134	TGGGAGCATTTTGGACAGGT	ATGCTGGGCTCCTTGTCTTC	tcgtcggcagcgtcagatgtgtataagagacagTGGGAGCATTTTGGACAGGT	gtctcgtgggctcggagatgtgtataagagacagATGCTGGGCTCCTTGTCTTC
Tgm3	MMG163	AAGACTACCTGTCCCCTCCC	AGAAGTCCATGTCTGGCAGC	tcgtcggcagcgtcagatgtgtataagagacagCATGTAGCCTGAGCCCTCTG	gtctcgtgggctcggagatgtgtataagagacagGGGTCGGTCACTCAGAGACA
Tgm3	MMG164	AAGACTACCTGTCCCCTCCC	AGAAGTCCATGTCTGGCAGC	tcgtcggcagcgtcagatgtgtataagagacagCATGTAGCCTGAGCCCTCTG	gtctcgtgggctcggagatgtgtataagagacagGGGTCGGTCACTCAGAGACA
Tgm3	MMG165	ATGCACAGGTTCCAGTGAGG	AAGGCTTTACCCATGGAGGC	tcgtcggcagcgtcagatgtgtataagagacagGAAGGGGAAGACAAGGAGCC	gtctcgtgggctcggagatgtgtataagagacagGTGAGCAACTCTTTTGGGCC
Tgm3	MMG166	ATGCACAGGTTCCAGTGAGG	AAGGCTTTACCCATGGAGGC	tcgtcggcagcgtcagatgtgtataagagacagGAAGGGGAAGACAAGGAGCC	gtctcgtgggctcggagatgtgtataagagacagGTGAGCAACTCTTTTGGGCC